

COMPARATIVE STUDY ON THE POSSIBLE EFFECT OF COD LIVER OIL VERSUS INSULIN ON PAROTID SALIVARY GLANDS OF STREPTOZOTOCIN-INDUCED DIABETIC ALBINO RATS

Amany A. Rabea*

ABSTRACT

Background: The diabetic condition is frequently associated with impaired functions of salivary glands, testified by both morphological deterioration of the gland and by altered salivary composition. Abnormal apoptosis has been implicated in salivary glands of diabetic rat models. Amyloidosis constitutes a group of diseases in which proteins deposit in tissues as insoluble fibrils, causing progressive organ dysfunction. Although insulin and oral hypoglycemic agents are the mainstays of diabetes treatment, they have prominent side effects and fail to alter the course of diabetic complications. Cod liver oil (CLO) is an important source of long-chain omega-3 (ω -3) fatty acids as well as vitamins A, E and D. CLO has antioxidant effect especially on parotid salivary glands.

Objective: The present study was undertaken to investigate the possible role of CLO versus insulin supplementation in enhancement of parotid salivary glands in streptozotocin (STZ)-induced diabetic rats.

Design: Sixty adult male Swiss albino rats (200-250 gm) were selected for this study. The animals were randomly divided into four groups (fifteen rats each): **Group I** (Control group), **Group II** (Diabetic untreated group), **Group III** (Insulin treated group) and **Group IV** (Cod liver oil treated group). At the end of the experimental period (four weeks), the rats were sacrificed and the parotid salivary glands were dissected out. The sections were examined histologically, immunohistochemically, histomorphometrically and by fluorescence staining technique. **Statistical analysis:** Data obtained from histomorphometric analysis were statistically described in terms of mean \pm standard deviation (\pm SD).

Results: Histopathologic examination of Group I showed the normal histological features of parotid gland. Group II revealed apparent reduction in acinar size, ill-defined acinar and ductal cells outlines, nuclear changes, acinar and ductal cells degeneration, lipid droplets, dilatation of the duct system lumina and stagnated salivary secretion in the lumina of striated and excretory ducts. Moreover apparent decrease, hyalinization and degeneration in the fibrous connective tissue (C.T)

* Lecturer, Oral Biology Department, Faculty of Oral and Dental Medicine, Future University.

fibroblasts showing signs of degeneration and dilated blood vessels (BVs) with swollen endothelial cells were noticed. Group III showed better histological features than those of Group II, while Group IV showed histological features resembling nearly those of the control group (Group I). The least immuno-expression for caspase-3 and the minimum fluorescence with thioflavin-T stain were demonstrated in Group I, followed by Group IV, then Group III and subsequently Group II. The histomorphometric analysis supported the previous results as Group I showed the highest mean acinar area fraction, followed by Group IV, then Group III and the least value was for Group II. On the other hand, Group I showed the least mean area percentage of both caspase-3 immunoreactivity and thioflavin-T fluorescence, followed by Group IV, then Group III and the highest values were for Group II. There was statistically highly significant difference between the studied groups.

Conclusions: Diabetes has deleterious effect on the structure and function of parotid salivary glands. Moreover, it has a major role in tissue damage through development of amyloidosis. Insulin can't completely inhibit the complications of diabetes. However, CLO has great potential to inhibit the abnormalities caused by diabetes.

KEY WORDS: Diabetes, parotid salivary gland, apoptosis, amyloidosis, insulin, cod liver oil.

INTRODUCTION

Diabetes mellitus (DM) is a metabolic disorder characterized by an impairment of carbohydrate, fat and protein metabolism caused by either lack of insulin secretion or decreased sensitivity of the tissues to insulin. This disease has reached epidemic levels in the United States and threatens a worldwide epidemic. The prevalence of diabetes is increasing rapidly and the disease incidence in 2010 was about 285 million people worldwide and is projected to increase to 438 million in 2030. There are two forms of DM: type 1 and 2. In type 1 diabetes or insulin-dependent DM, the pancreatic β -cells are progressively destroyed and secrete little or no insulin. Type 2 diabetes or non-insulin-dependent DM, is a heterogeneous disorder of insulin resistance and pancreatic β -cell dysfunction (*American Diabetes Association, 2009; Chapple and Genco, 2013*).

The diabetic condition is frequently associated with retinopathy, nephropathy, neuropathy, cardiovascular disease and peripheral vascular disease (*Kidambi and Patel, 2008*). Often periodontal disease, gingivitis, tongue inflammation, oral candidiasis, dental caries and xerostomia also afflict patients with diabetes. These disorders are

generally accompanied with impaired functions of salivary glands, testified by both morphological deterioration of the glandular parenchyma and by altered salivary composition (*Carda et al., 2006; Negrato and Tarzia, 2010*). Several reports document altered concentration of proteins such as amylase, lactoferrin and proline-rich protein in diabetic saliva (*Aydin, 2007*). Furthermore, salivary proteins synthesis is influenced by hyperglycemia which causes post-translational disorders (*Hirtz et al., 2006; Wong, 2006; Rao et al., 2009; Gregersen and Bross, 2010*).

The term apoptosis is given to a morphologically distinct mode of cell death. In terms of tissue kinetics, apoptosis might be considered a mechanism that counterbalances the effect of cell proliferation by mitotic division. On the other hand, excessive apoptosis might cause organ atrophy and failure. Apoptosis plays an important role in several diabetic complications. These include apoptosis of neuronal cells in diabetic neuropathy, myocardial apoptosis which plays a role in cardiac pathogenesis and apoptosis of mesangial cells that occurs in diabetic nephropathy. Furthermore, abnormal apoptosis has been implicated in salivary glands of diabetic rat models. The molecular events regulating apoptosis are complex and involve genes that are

both pro-apoptotic and anti-apoptotic. Caspases, a family of cysteine proteases, are integral parts of the apoptotic pathway. To date, 14 caspases have been implicated in the apoptotic pathway cascade. Among these, caspase-3 is considered to be a major execution protease. Caspase-3, in particular, has many cellular targets and when it is activated, it produces morphologic features of apoptosis (*Take et al., 2007; Shredah and El-Sakhawy, 2014*).

Amyloidosis constitutes a group of diseases in which proteins deposit in tissues as insoluble fibrils, causing progressive organ dysfunction. About, 25 structurally unrelated proteins are known to cause amyloidosis. For each of these amyloidogenic “precursor proteins,” the initial step in amyloid fibril formation is a misfolding event. The misfolding can result from proteolytic cleavage (*e.g.*, amyloid β protein), an amino acid substitution (*e.g.*, transthyretin [TTR]) or intrinsic properties that become significant only at high serum concentration or in the presence of specific local factors (*e.g.*, β 2-microglobulin [β 2m]), (*Merlini and Bellotti, 2003; Westermarck et al., 2005*). Classification of the amyloidosis is based on the precursor protein that forms the amyloid fibrils and the distribution of amyloid deposition as either systemic or localized. The major types of systemic amyloidosis are immunoglobulin (Ig) light chain (AL), Ig heavy chain (AH), amyloid A (AA), the familial or hereditary amyloidosis (TTR, fibrinogen A α , lysozyme, apolipoprotein AI [apoAI], apoAII, gelsolin and cystatin), senile systemic amyloidosis and β 2m amyloidosis (*Skinner et al., 2004; Obici et al., 2005*). It was reported by some studies the relationship between diabetes type 2 and the development of amyloidosis (*Border et al., 2012; Iannuzzi et al., 2015*). Amyloid fibrils stain with dyes such as thioflavin-T producing a characteristic apple green birefringence when visualized under fluorescence microscope (*Fabian et al., 2008*).

Although insulin and oral hypoglycemic agents are the mainstays of diabetes treatment, they have prominent side effects and fail to alter the course of diabetic complications. Hypoglycemia and complications in macrovascular and retinal functions in addition to neuropathic problems are still associated in the patients receiving insulin. Moreover, it has been shown that insulin is unable to completely inhibit protein glycation which can maintain increased oxidative stress in diabetic tissues. These problems led several investigators to focus their attention on the traditional medicines (*Jain et al., 2006*).

Food derived antioxidants have a strong potential for long term use as chemo-preventive agents in disease states involving oxidative stress (*Mckim et al., 2002*). There is low prevalence of diabetes in people living in Faeroe Islands, Alaskan Eskimos and the Greenland (*Simonsen et al., 1987; Burrows et al., 2000; Jorgensen et al., 2002*). The lower prevalence of diabetes in these populations was due to their higher intake of omega-3 (ω -3) or (n-3) rich fish and marine mammals (*Jorgensen et al., 2002*). Fish oil (FO) is a compound rich in ω -3 fatty acids which are polyunsaturated fatty acids (PUFAs) mainly represented by eicosapentaenoic acid (EPA) and docosahexaenoic acid (DHA) that regulate a wide range of functions in the body including blood pressure, blood clotting, modulation of inflammatory response as well as correct development and functioning of brain and nervous systems. Epidemiological studies suggest that among populations ingesting large amounts of PUFAs, mainly present in FO, there are reduced risk of neurodegenerative disorders such as Alzheimer’s disease, lower incidence of acute myocardial infarction and chronic inflammatory diseases such as rheumatoid arthritis, ulcerative colitis and psoriasis among other inflammatory diseases (*Lordan et al., 2011*). Additionally, it has been tested an increased intake of ω -3 fatty acids might reduce the risk of developing diabetes in mice received streptozotocin (STZ), (*Soltan, 2012*).

Among the different types of FO, cod liver oil (CLO) is an important source of long-chain ω -3 fatty acids (EPA & DHA) as well as vitamins A, E and D. Oral administration of CLO improved the deleterious effects of alloxan-induced diabetic rats (*Hamdy et al., 2007*). Moreover, it was reported that CLO has antioxidant effect especially on parotid glands where an increase of glutathione and catalase activities was reported. Furthermore, an increase of catalase activity in submandibular salivary glands was noticed after CLO administration (*Leite et al., 2014*).

From this light, the present study was undertaken to investigate the possible role of CLO versus insulin supplementation in enhancement of parotid salivary glands in STZ-induced diabetic rats.

MATERIALS AND METHODS

Animals

Sixty adult male Swiss albino rats (200-250 gm) were selected for this study. The steps of experiment were done according to the rules approved by the Bio-ethical Committee of Faculty of Dentistry, Ain-Shams University. The rats were housed in separate metal cages, five rats per cage in Ain-Shams animal house under controlled temperature, humidity and dark-light cycle. The size of the cage was 20 cm width and 40 cm length. This was done under supervision of specialized veterinarian since their housing till getting rid of sacrificed bodies which was done by the incinerator of Ain-Shams. Rats were kept under good ventilation and adequate stable diet consisting of fresh vegetables, dried bread and tap water throughout the experimental period.

Experimental procedure

After one week acclimatization period, the animals were randomly divided into four groups (fifteen rats each):

Group I (Control group): The rats of this group received a single intraperitoneal injection of 1 ml/kg body weight citrate buffer (0.1 M; pH 4.5) under ether anesthesia (*Anu Geethan and Prince, 2008*).

Group II (Diabetic untreated group): The rats were fasted for 14 h and diabetes was induced by a single intraperitoneal injection of 40 mg/kg body weight STZ (Sigma Chemical Co., St. Louis, MO, USA) freshly dissolved in 1 ml/kg body weight citrate buffer (0.1 M; pH 4.5) under ether anesthesia. After the injection, the animals were given free access to water and food. Blood samples were obtained via vein puncture of tail vein. Fasting glycemia was measured by the glucose oxidase method using a clinical glucometer. Plasma glucose level greater than 300 mg/dl confirmed the occurrence of diabetes that was determined three days after the drug injection (*Anu Geethan and Prince, 2008*).

Group III (Insulin treated group): After confirmation of diabetes, rats received subcutaneous injection of human insulin (rDNA), (Mixtard[®] 30, Novo Nordisk, Denmark) with a dose (5 IU/kg body weight/day) for four weeks. The rats received the last insulin dose 24 hours before being sacrificed (*Pinheiro et al., 2011*).

Group IV (Cod liver oil treated group): After confirmation of diabetes, rats received pure cod liver oil (Arctic Cod Liver Oil[®], Nordic Naturals, Inc., USA) with a dose (60 mg/Kg body weight/day) by intra-gastric intubation for four weeks (*Marjan et al., 2012*).

Animal sacrifice

At the end of the experimental period which was four weeks for all groups, the animals were sacrificed by ketamine over dose (*Shredah and El-Sakhawy, 2014*).

Specimen preparation

Hematoxylin and Eosin (H&E) staining

The parotid salivary glands were dissected out and fixed immediately in 10% neutral buffered formalin solution. Then the specimens were washed by tap water, dehydrated in ascending grades of ethyl alcohol, cleared in xylene and embedded in paraffin wax. Sections of 4-5 μm in thickness were obtained and mounted on clean glass slides. Tissue sections were then deparaffinized in xylene and rehydrated by ethanol series ending with pure H₂O (Millipore Corporation, Temecula, CA, USA) before histological staining with H&E solutions (Sigma, St. Louis, MO, USA), to verify histological details (*Shredah and El-Sakhawy, 2014*).

Immunohistochemistry

Immunolabeling for detection of caspase-3 was performed on paraffin sections of 4-5 μm in thickness mounted on positively charged microscope slides. The set of sections were incubated in hot oven for 2 hours at 56°C, deparaffinized in xylene and rehydrated by ethanol series ending with pure H₂O (Millipore Corporation, Temecula, CA, USA). After 5 minutes washing in phosphate buffered saline (PBS), sections were incubated in 0.05 mg/ml proteinase K in 0.05 M Tris-HCl, 0.01 M Ethylene diamine tetra acetic acid (EDTA) and 0.01 M NaCl, pH 7.8 for 10 minutes at 37°C. After two washes with PBS, unmasking of the antigens was carried out using antigen retrieval citrate buffer solution for 10 minutes in boiling water. Then the sections were placed in a humid chamber and the endogenous tissue peroxidase was blocked with 3% hydrogen peroxide for 5 minutes. Incubation with bovine serum albumin for 20 minutes was performed to reduce unwanted nonspecific reactions. Without washing, the sections were incubated with the primary antibody overnight at 4°C. The primary antibody used was

anti-caspase-3 active form (Millipore Corporation, Temecula, CA, USA) with dilution 1:100. In the next day, after washing in PBS, the sections were incubated with secondary universal antibody (Vectastain Universal Elite ABC-peroxidase kit, Vector Laboratories) and then with the Avidin-Biotin complex (ABC) (Vectastain Universal Elite ABC kit, Vector Laboratories, Burlingame, CA, USA) according to the manufacturer's protocol. The substrate 3,3'-diaminobenzidine (DAB) was applied for the same amount of time on all labeled sections until development of desired brown color. Finally, the sections were counter-stained with Mayer's hematoxylin (Sigma, St. Louis, MO, USA) for 30 seconds to visualize tissue topography. The negative control was obtained by omitting the primary antibody from the protocol outlined above (*Shredah and El-Sakhawy, 2014*).

Histological and immunohistochemical examinations were performed using light microscope (Olympus® BX 60, Tokyo, Japan) at (400 x) magnification.

Fluorescence staining

A set of sections from each group was stained using thioflavin-T (Sigma, St. Louis, MO, USA) to detect amyloid fibrils aggregation. Sections were incubated in hot oven for 15 minutes at 60°C, deparaffinized in xylene and rehydrated in descending grades of ethanol to water. After washing in PBS, the sections were incubated with thioflavin-T solution (0.5% thioflavin-T in 0.1N HCl) at room temperature away from light for 10 minutes. The sections thereafter, were rinsed sequentially in PBS and deionized water (for 5 minutes each) and then cover slipped. In the absence of amyloid fibrils, the dye fluoresced faintly at the excitation and emission maximum of 350 and 438 nm, respectively. In the presence of amyloid fibrils, there was a bright fluorescence with this dye at the excitation and emission maximum of

450 and 482nm, respectively (*Shen et al., 2011*). All sections were examined under a dark field ultraviolet fluorescence microscope (Olympus®, BX41, Tokyo, Japan) at (400 x) magnification.

Histomorphometric analysis

The data were obtained using Leica Qwin 500 image analyzer computer system (England). The image analyzer consisted of a coloured video camera, coloured monitor, hard disc of IBM personal computer connected to the microscope and controlled by Leica Qwin 500 software. The image analyzer was first calibrated automatically to convert the measurement units (pixels) produced by the image analyzer program into actual micrometer (μm) units.

In H&E stained sections, the image analysis system was used to assess the acinar area fraction (percentage). In the immunohistochemistry treated sections and fluorescence stained sections, the image analysis system was used to assess the area percentage of caspase-3 immunoreactivity and thioflavin-T positive staining respectively, in parenchymal elements and connective tissue (C.T) of the studied specimens. After grey calibration, the image was transformed into a grey delineated image to choose areas exhibiting positive reactivity/staining with accumulation of all grades of reactivity/staining (minimum, maximum and median grey). Areas of positive reaction/staining were then masked by a blue binary color. Ten fields were measured for each specimen. The studied fields were measured under magnification 40x objective lens. Mean values were obtained for each specimen. All the calculations were performed in relation to a standard measuring frame of an area $118476.6 \mu\text{m}^2$.

Statistical analysis

Data obtained from histomorphometric analysis were statistically described in terms of mean \pm standard deviation (\pm SD). One-way analysis of variance (ANOVA) test was used to compare

between the four groups followed by Tukey's post hoc test. A probability value (P-value) <0.001 was considered as highly significant and P-value ≤ 0.05 was considered significant. Statistical analysis was performed by Microsoft® Excel 2013 (Microsoft® Corporation, NY, USA) and Statistical Package for the Social Science (SPSS® Inc., Chicago, IL, USA) version 20.

RESULTS

Histological results

Group I (Control group)

Histopathologic examination of Group I showed the C.T septa dividing the gland into lobes and lobules. Normal histological features of parenchymal elements were noticed. The terminal end piece of the parotid gland was formed of serous acini. The serous acini were more or less spherical in shape. Each acinus was composed of pyramidal cells, with their apices occupied with eosinophilic stained granules situated toward a central apparently narrow lumen. The cytoplasm stained moderately basophilic. The nuclei were apparently large, spherical and occupying the basal third of the cells. Intercalated ducts were found intralobular, lined by cuboidal cells with basophilic cytoplasm and centrally placed apparently large rounded nuclei filling most of the cells. Their lumina were apparently larger than those of the acini (**Fig. 1a**).

The striated ducts were found intralobular. They appeared more or less rounded and lined by columnar cells with prominent eosinophilic basal striations. The cytoplasm appeared eosinophilic with centrally situated nuclei (**Fig. 2a**).

The excretory ducts were observed interlobular, apparently large in size and lined by pseudostratified columnar epithelial cells. The ducts lumina showed apparently varied diameters. The ducts were surrounded by fibrous C.T stroma. Neighboring

blood vessels (BVs) adjacent to the ducts were lined by thin endothelial cells (**Fig. 3a**).

Group II (Diabetic untreated group)

Examining the H&E stained sections of this group revealed serous acini with apparent reduction in size. The acinar cells showed ill-defined outline in addition, some acinar cells undergo degeneration leaving spaces between them. Serous cells were extensively invaded by lipid droplets of apparently various sizes which sometimes gave a honeycomb appearance. The cells nuclei appeared hyperchromatic and pleomorphic. Many nuclei were displaced by lipid droplets and some of them had crescent shape. Furthermore, many nuclei were pyknotic while some were karyolytic. However, few nuclei undergo karyorrhexis and others with marginated chromatin were observed. Dilated BVs as well as few extravasated red blood cells (RBCs) were also noticed between the acini. Intercalated ducts lumina were dilated on the expense of cell height. The ductal cells nuclei were displaced in addition, some of them were hyperchromatic and had crescent shape. Moreover, some nuclei were pyknotic while few were karyolytic. Degenerated ductal cells could be observed (**Fig. 1b**).

Some of striated duct cells appeared with ill-defined boundaries and apparent decrease in the columnar appearance together with loss of basal striations. However, some columnar cells with basal striations were detected. Lipid droplets were observed within some ductal cells. Furthermore, some cells showed signs of complete degeneration. Pyknotic and hyperchromatic as well as karyolytic nuclei were detected in some ductal cells. Lumina of some striated ducts were dilated with desquamated cells and stagnated secretion infiltrated by lipid droplets could be noticed (**Fig. 2b**).

The excretory ducts showed dilated lumen on expense of cell height. Moreover, excretory duct cells showed loss of pseudostratification.

Some lining cells nuclei were pyknotic, others were hyperchromatic and few were karyolytic. Furthermore, cells with signs of degeneration as well as lipid droplets were detected. Stagnated secretion with desquamated cells and extensive infiltration by apparently small sized lipid droplets which gave a granular appearance was observed in the lumen of some ducts. However, homogenous stagnated secretion with apparently large sized lipid droplets was observed in other ducts. The BVs adjacent to the excretory ducts were dilated, lined by swollen endothelial cells and engorged with RBCs. Few extravasated RBCs between the acini could be detected. Apparent decrease in the fibrous C.T surrounding the excretory ducts together with inflammatory cells infiltration could be observed. In addition, areas of hyalinization with fibroblasts showing signs of degeneration were apparent. Moreover, apparently large areas of degeneration in the C.T could be detected (**Fig. 3b**).

Group III (Insulin treated group)

Examining the H&E stained sections of this group revealed some serous acini with apparent reduction in size. Some acinar cells showed ill-defined outline however, few acinar cells undergo degeneration leaving spaces between them. Some acinar cells showed apparently different sized lipid droplets. Some cells nuclei appeared hyperchromatic and pleomorphic, while others appeared normal. Some nuclei were pyknotic, while others were displaced by lipid droplets and had crescent shape. Few nuclei were karyolytic and few showed karyorrhexis. Furthermore, marginated chromatin was detected in few nuclei. Few extravasated RBCs were also noticed between the acini. Intercalated ducts lumina were lined by cuboidal cells. Some duct cells nuclei were pyknotic and hyperchromatic, few were karyolytic and others showed marginated chromatin. Duct cells with signs of degeneration could be observed (**Fig. 1c**).

Few striated duct cells showed ill-defined boundaries and apparent decrease in the columnar

appearance together with loss of basal striations. However, many columnar cells with basal striations were detected. Few lipid droplets were observed within some ductal cells. Furthermore, few cells showed signs of complete degeneration. Pyknotic and hyperchromatic nuclei in addition to karyolytic nuclei were detected in some ductal cells. Lumina of some striated ducts with stagnated secretion infiltrated by lipid droplets could be observed (**Fig. 2c**).

Most of the excretory duct cells were pseudostratified columnar epithelial cells. However, some cells showed apparent decrease in cell height as well as loss of pseudostratification. Few lining cells nuclei were pyknotic and hyperchromatic. Furthermore, few lipid droplets were detected within the cells. Desquamated cells were observed in the duct lumen. The BVs adjacent to the excretory ducts appeared somewhat dilated, lined by somewhat swollen endothelial cells and engorged with RBCs. There was apparent increase of the fibrous C.T surrounding the excretory ducts. Some inflammatory cells infiltration and Russell bodies were noticed. Areas of hyalinization with few fibroblasts showing signs of degeneration could be detected. Moreover, apparently large areas of degeneration in the C.T could be observed (**Fig. 3c**).

Group IV (Cod liver oil treated group)

Histopathologic examination of Group IV showed histological features resembling nearly those of the control group. The serous acini were more or less spherical in shape. Each acinus was composed of pyramidal cells, with their apices occupied with eosinophilic stained granules situated toward a central apparently narrow lumen. The cytoplasm stained moderately basophilic. Most of nuclei were

apparently large, spherical and occupying the basal third of the cell however, few were pleomorphic. Furthermore, few pyknotic and hyperchromatic nuclei as well as karyolytic nuclei were detected. Few serous cells were invaded by apparently small sized lipid droplets. Intercalated ducts were found intralobular, lined by cuboidal cells with basophilic cytoplasm and centrally placed apparently large rounded nuclei filling most of the cells. However, few karyolytic nuclei and others with marginated chromatin were detected. The ducts lumina were apparently larger than those of the acini (**Fig. 1d**).

The striated ducts were found intralobular. They were lined by columnar cells with prominent eosinophilic basal striations. The cytoplasm appeared intensely eosinophilic with centrally situated nuclei. However, apparently small lipid droplets as well as pyknotic and hyperchromatic nuclei were observed within few ductal cells. Most of the ducts lumina showed no stagnated secretion except few striated ducts lumina were filled by stagnated secretion infiltrated by lipid droplets could be observed (**Fig. 2d**).

The excretory ducts were observed interlobular, apparently large in size and lined by pseudostratified columnar epithelial cells except few areas which showed loss of pseudostratification. Pyknotic and hyperchromatic nuclei as well as apparently small lipid droplets within few cells were detected. The ducts lumina were empty and showed apparently varied diameters. The ducts were surrounded by fibrous C.T stroma with some inflammatory cells infiltration. Moreover, apparently small areas of degeneration in the C.T could be observed. The neighboring BVs adjacent to the ducts had apparently small diameter and they were lined by thin endothelial cells (**Fig. 3d**).

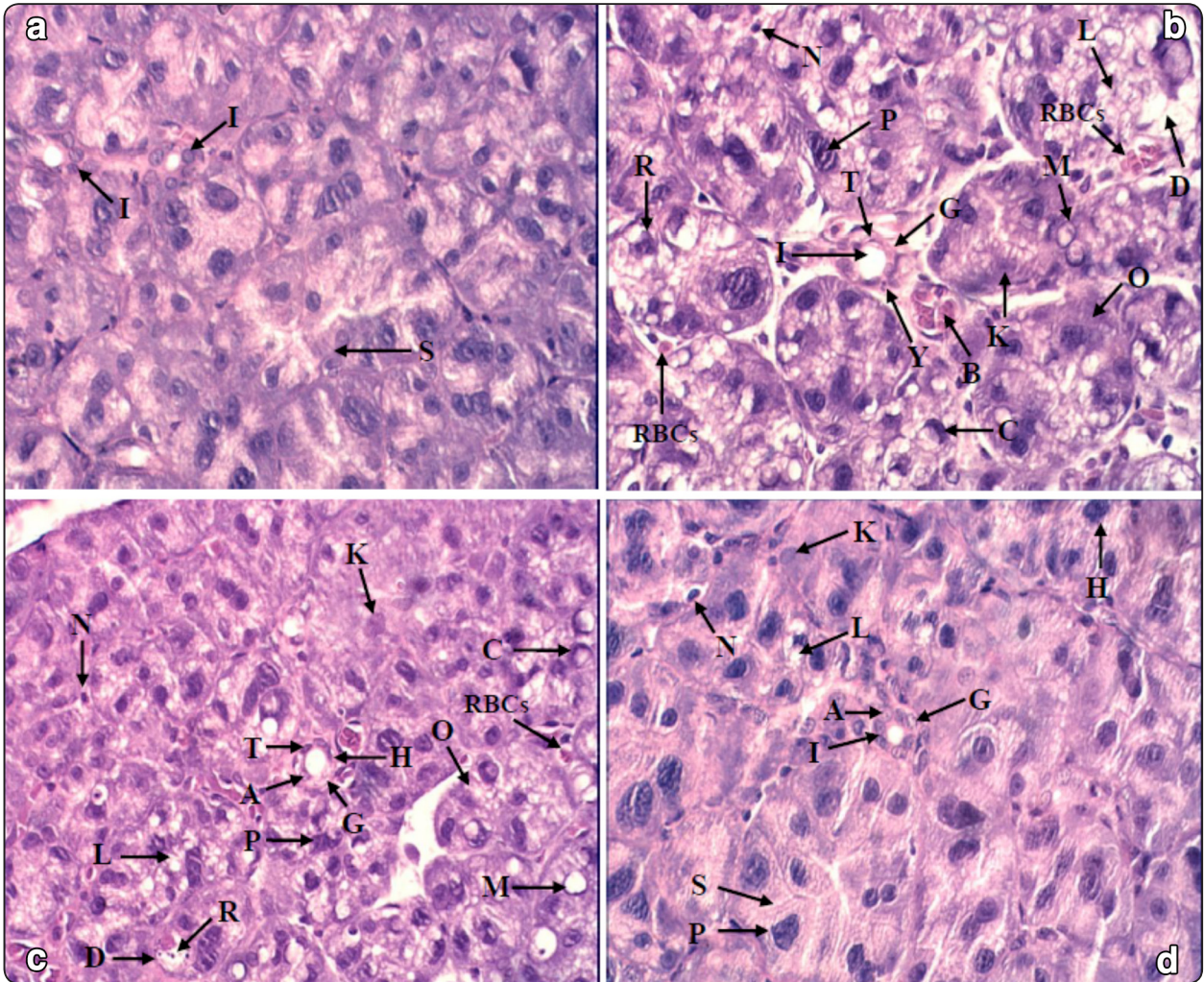


Fig. (1): Photomicrographs of H&E sections: (a)- Control group (I) showing: normal architecture of serous acini (S) and intercalated ducts (I), (the original magnification x400). (b)- Diabetic untreated group (II) showing: serous acini with apparent reduction in size. Acinar cells with ill-defined outline (O). Acinar cells undergo degeneration (D). Lipid droplets with honeycomb appearance (L). Hyperchromatic and pleomorphic nuclei (P). Nuclei have crescent shape (C). Pyknotic (N) and karyolytic (K) nuclei. Few nuclei undergo karyorrhexis (R) and others with marginated chromatin (M). Dilated BVs (B) and extravasated RBCs. Dilated intercalated duct lumen (I). Hyperchromatic ductal cells nuclei that have crescent shape (T). Pyknotic nuclei (Y). Karyolytic nuclei in degenerated ductal cells (G), (the original magnification x400). (c)- Insulin treated group (III) showing: some serous acini with apparent reduction in size. Acinar cells with ill-defined outline (O). Acinar cells undergo degeneration (D). Apparently different sized lipid droplets (L). Hyperchromatic and pleomorphic nuclei (P). Pyknotic nuclei (N) and others have crescent shape (C). Karyolytic nuclei (K), nuclei show karyorrhexis (R) and others have marginated chromatin (M). Extravasated RBCs. Intercalated duct cells nuclei are pyknotic and hyperchromatic (T). Karyolytic nuclei (A) and others show marginated chromatin (H). Duct cells with signs of degeneration (G), (the original magnification x400). (d)- Cod liver oil treated group (IV) showing: nearly normal architecture of serous acini (S). However, few nuclei are pleomorphic (P). Few pyknotic (N) and hyperchromatic (H) nuclei as well as karyolytic (K) nuclei are detected. Apparently small sized lipid droplets (L). Nearly normal architecture of intercalated duct (I). However, few karyolytic nuclei (A) and others with marginated chromatin (G) are detected, (the original magnification x400).

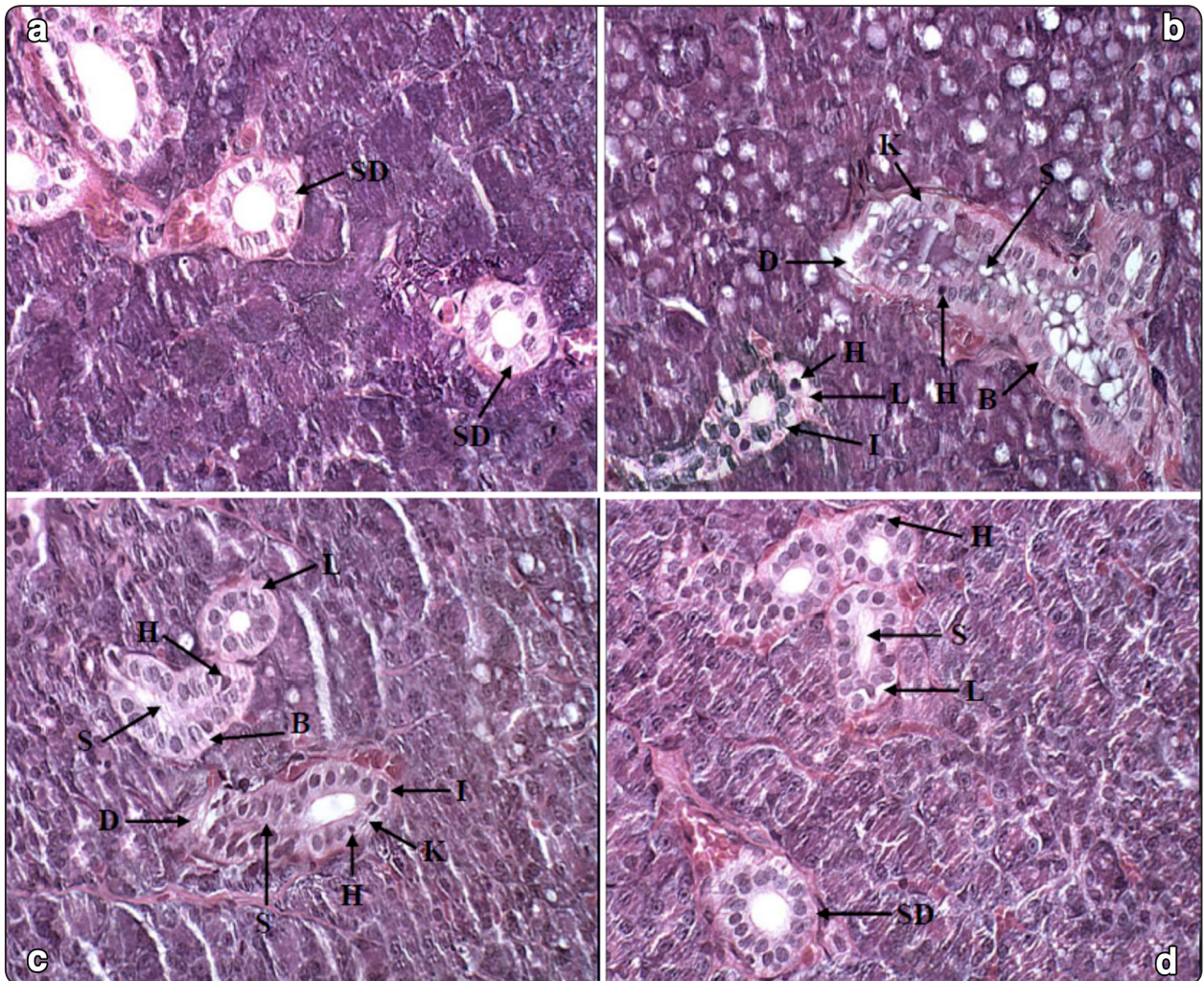


Fig. (2): Photomicrographs of H&E sections: (a)- Control group (I) showing: normal architecture of the striated ducts (SD), (the original magnification x400). (b)- Diabetic untreated group (II) showing: striated duct cells with ill-defined boundaries, apparent decrease in the columnar appearance and loss of basal striations (I). Some columnar cells with basal striations (B). Lipid droplets (L). Cells with signs of complete degeneration (D). Pyknotic and hyperchromatic (H) as well as karyolytic (K) nuclei. Lumina of some striated ducts are dilated with desquamated cells and stagnated secretion infiltrated by lipid droplets (S), (the original magnification x400). (c)- Insulin treated group (III) showing: striated duct cells with ill-defined boundaries, apparent decrease in the columnar appearance and loss of basal striations (I). Many columnar cells with basal striations (B). Lipid droplets (L). Cells with signs of complete degeneration (D). Pyknotic and hyperchromatic (H) as well as karyolytic (K) nuclei. Lumina of some striated ducts with stagnated secretion infiltrated by lipid droplets (S), (the original magnification x400). (d)- Cod liver oil treated group (IV) showing: nearly normal architecture of the striated ducts (SD). However, apparently small lipid droplets (L), pyknotic and hyperchromatic nuclei (H) are observed. Few striated ducts lumina are filled by stagnated secretion infiltrated by lipid droplets (S), (the original magnification x400).

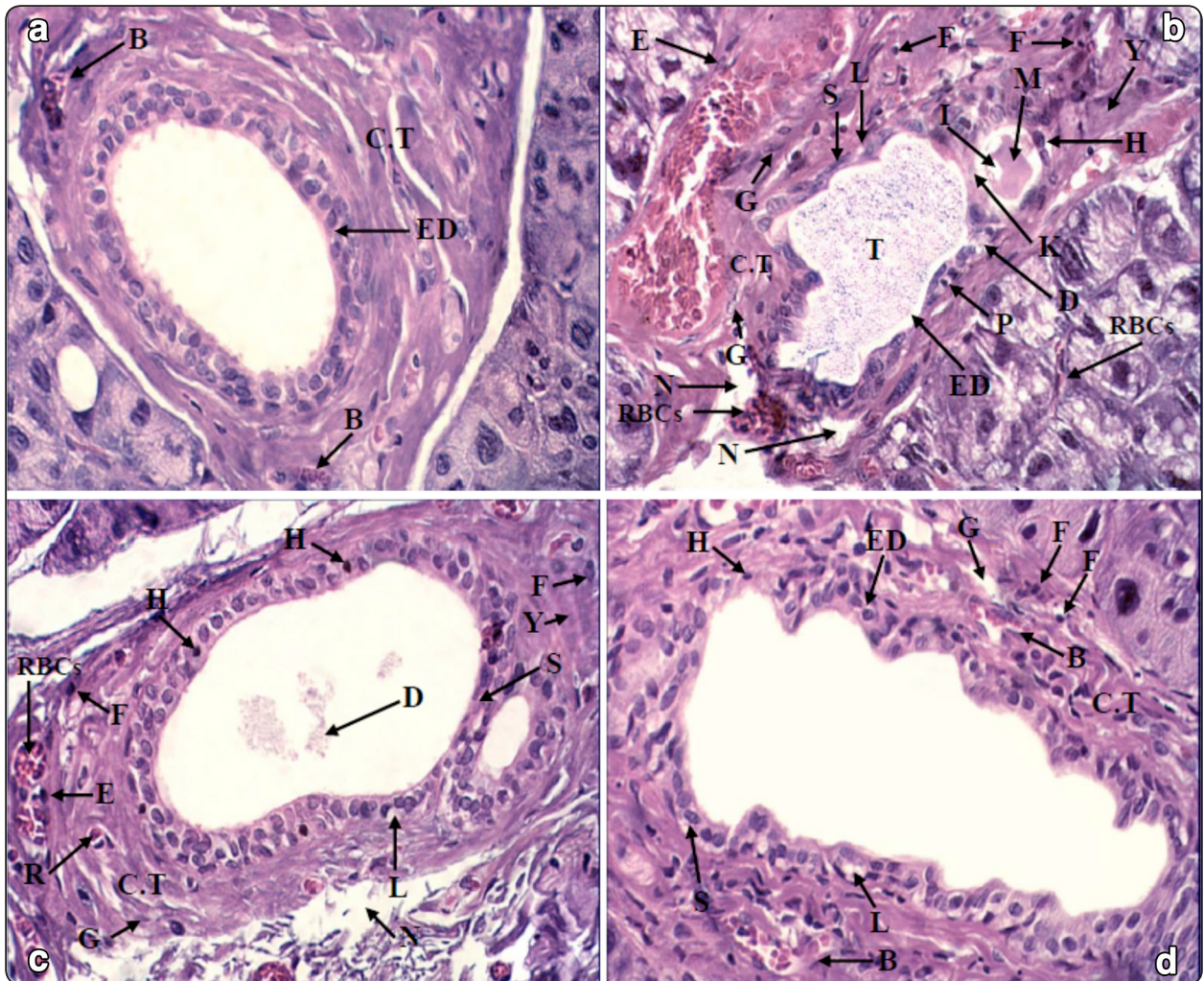


Fig. (3): Photomicrographs of H&E sections: (a)- Control group (I) showing: normal architecture of the excretory duct (ED) surrounded by fibrous C.T stroma. Normal BVs (B), (the original magnification x400). (b)- Diabetic untreated group (II) showing: excretory ducts with dilated lumina (ED). Loss of cells pseudostratification (S). Pyknotic (P), hyperchromatic (H) and few karyolytic (K) nuclei. Cells with signs of degeneration (D). Lipid droplets (L). Stagnated secretion with desquamated cells and apparently small sized lipid droplets which give a granular appearance (T). Homogenous stagnated secretion (M) with apparently large sized lipid droplets (I). The dilated BVs are lined by swollen endothelial cells (E) and engorged with RBCs. Extravasated RBCs. Apparent decrease in the fibrous C.T. Inflammatory cells infiltration (F). Areas of hyalinization (Y) and fibroblasts showing signs of degeneration (G). Apparently large areas of degeneration (N) in the C.T, (the original magnification x400). (c)- Insulin treated group (III) showing: excretory ducts with loss of cells pseudostratification (S). Pyknotic and hyperchromatic (H) nuclei. Few lipid droplets (L). Desquamated cells (D) in the duct lumen. Somewhat dilated BVs are lined by somewhat swollen endothelial cells (E) and engorged with RBCs. Apparent increase of the fibrous C.T. Some inflammatory cells infiltration (F) and Russell bodies (R). Areas of hyalinization (Y) and few fibroblasts showing signs of degeneration (G). Apparently large areas of degeneration (N) in the C.T, (the original magnification x400). (d)- Cod liver oil treated group (IV) showing: nearly normal architecture of the excretory duct (ED). However, few areas show loss of pseudostratification (S). Few pyknotic and hyperchromatic (H) nuclei. Apparently small lipid droplets (L). Some inflammatory cells infiltration (F). Apparently small areas of degeneration (G) in the C.T. The BVs have apparently small diameter and lined by thin endothelial cells (B), (the original magnification x400).

Immunohistochemical results

Nuclear and/or cytoplasmic caspase-3 expressions were detected in the acinar and ductal cells as well as the C.T cells of Groups I, II, III and IV with different patterns of reactivity.

In Group I, the cells of secretory acini and duct system together with the C.T cells as well as the endothelial cells showed negative nuclear immunohistochemical expression for caspase-3 however, mild expression was observed in the cytoplasm of few cells (Figs. 4a, 5a & 6a). On contrary, in Group II a strong immuno-expression for caspase-3 was observed in the nuclei and cytoplasm of acinar and ductal cells, the C.T cells as well as

the endothelial cells (Figs. 4b, 5b & 6b). In Group III, moderate immuno-expression for caspase-3 was detected in few nuclei and in the cytoplasm of the secretory acini and intercalated duct cells, while moderate immuno-expression was detected in most of the nuclei and in the cytoplasm of the striated duct and excretory duct cells, the C.T cells as well as the endothelial cells (Figs. 4c, 5c & 6c). On the other hand, in Group IV mild immuno-expression for caspase-3 was detected in the cytoplasm of the acinar and ductal cells, the C.T cells as well as the endothelial cells, while negative nuclear immuno-expression was observed in the previous mentioned elements (Figs. 4d, 5d & 6d).

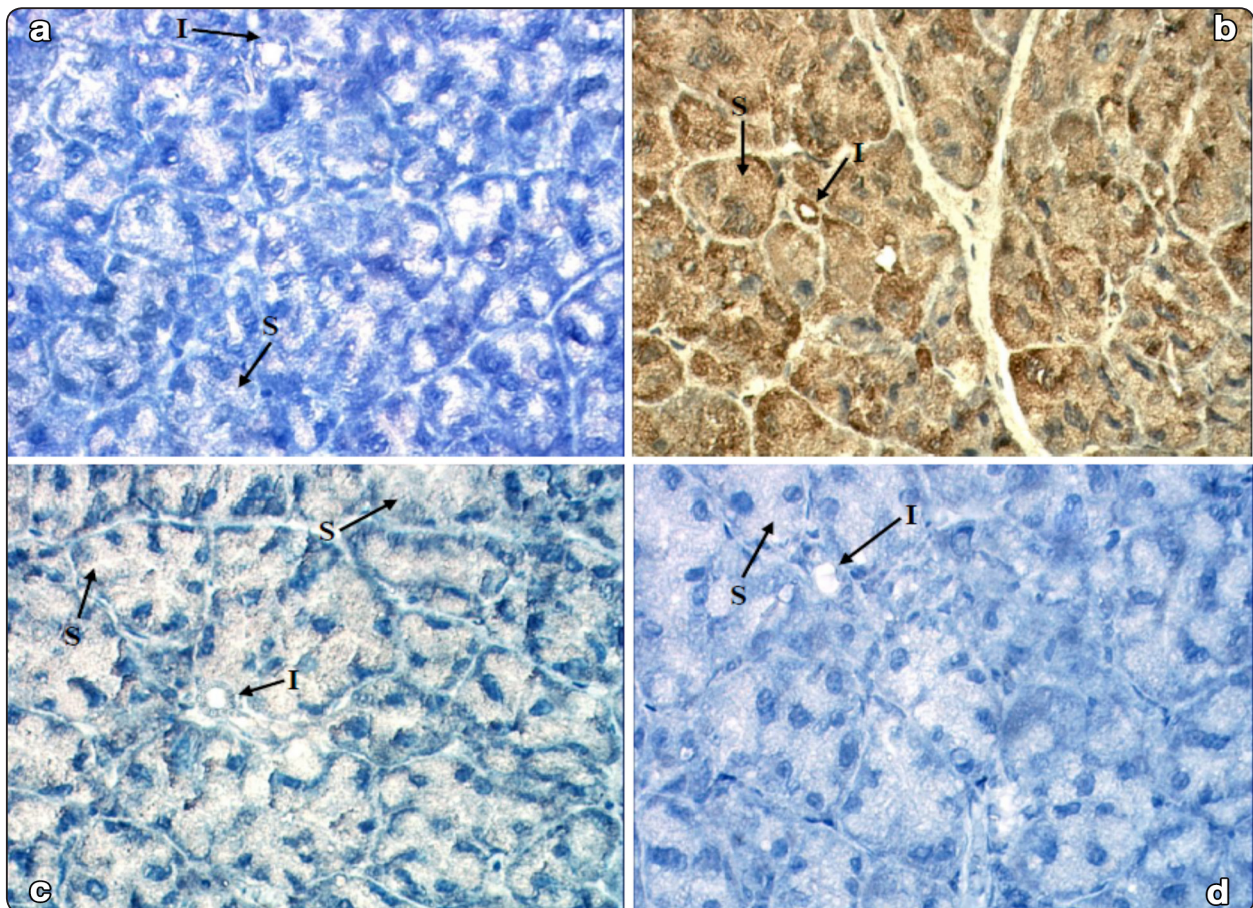


Fig. (4): Photomicrographs of caspase-3 immunolocalization: (a)- Control group (I) showing: the cells of secretory acini and intercalated duct have negative nuclear immunohistochemical expression for caspase-3 however, mild expression is observed in the cytoplasm of few acinar (S) and ductal (I) cells, (the original magnification x400). (b)- Diabetic untreated group (II) showing: a strong immuno-expression for caspase-3 in the nuclei and cytoplasm of acinar cells (S) and intercalated duct cells (I), (the original magnification x400). (c)- Insulin treated group (III) showing: moderate immuno-expression for caspase-3 in few nuclei and in the cytoplasm of the secretory acini (S) and intercalated duct cells (I), (the original magnification x400). (d)- Cod liver oil treated group (IV) showing: negative nuclear immuno-expression for caspase-3 but mild immuno-expression in the cytoplasm of the acinar cells (S) and intercalated duct cells (I), (the original magnification x400).

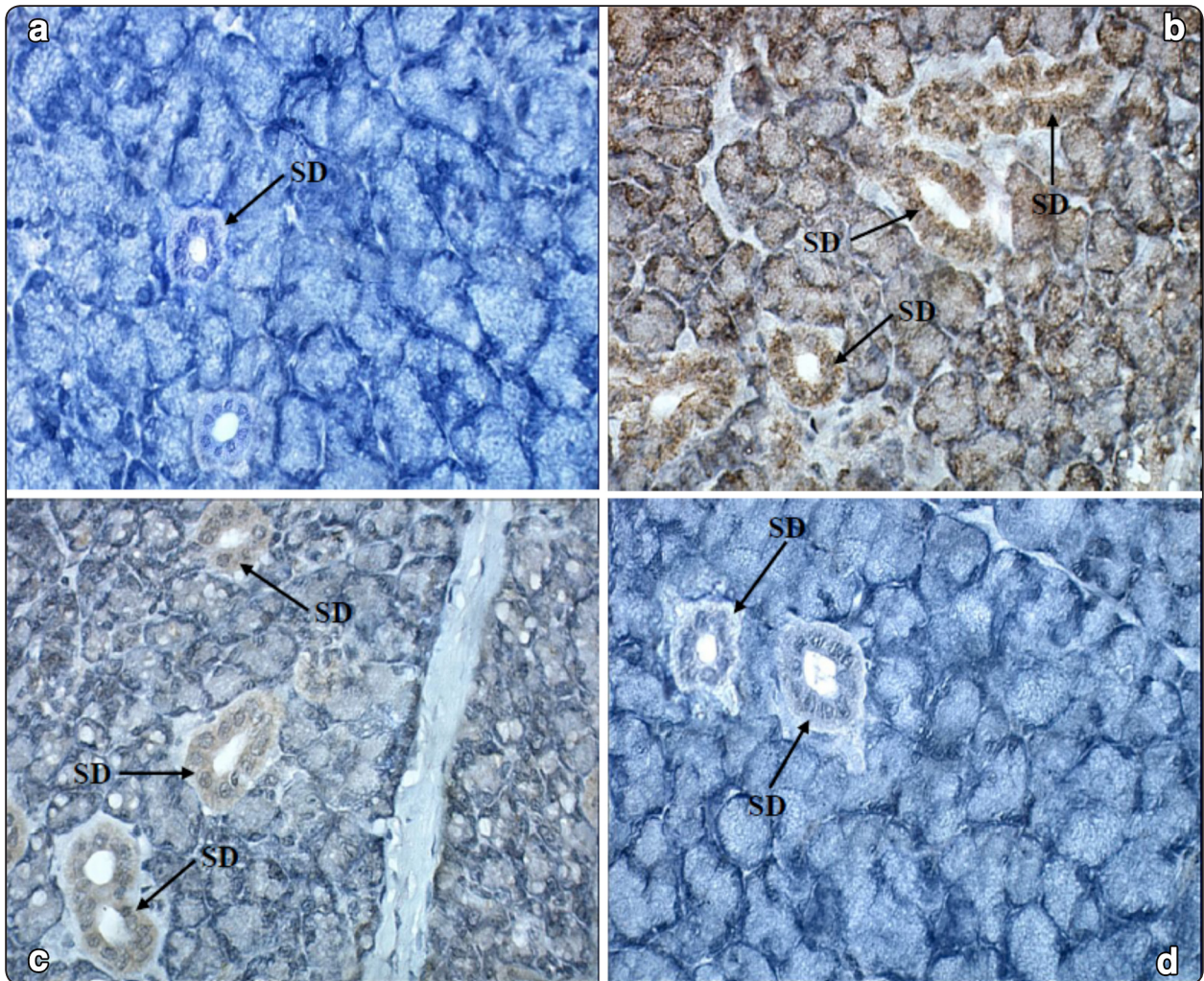


Fig. (5): Photomicrographs of caspase-3 immunolocalization: (a)- Control group (I) showing: striated duct cells have negative nuclear immunohistochemical expression for caspase-3 however, mild expression is observed in the cytoplasm of few cells (SD), (the original magnification x400). (b)- Diabetic untreated group (II) showing: a strong immuno-expression for caspase-3 in the nuclei and cytoplasm of striated duct cells (SD), (the original magnification x400). (c)- Insulin treated group (III) showing: moderate immuno-expression for caspase-3 in most of the nuclei and in the cytoplasm of the striated duct cells (SD), (the original magnification x400). (d)- Cod liver oil treated group (IV) showing: negative nuclear immuno-expression for caspase-3 but mild immuno-expression in the cytoplasm of the striated duct cells (SD), (the original magnification x400).

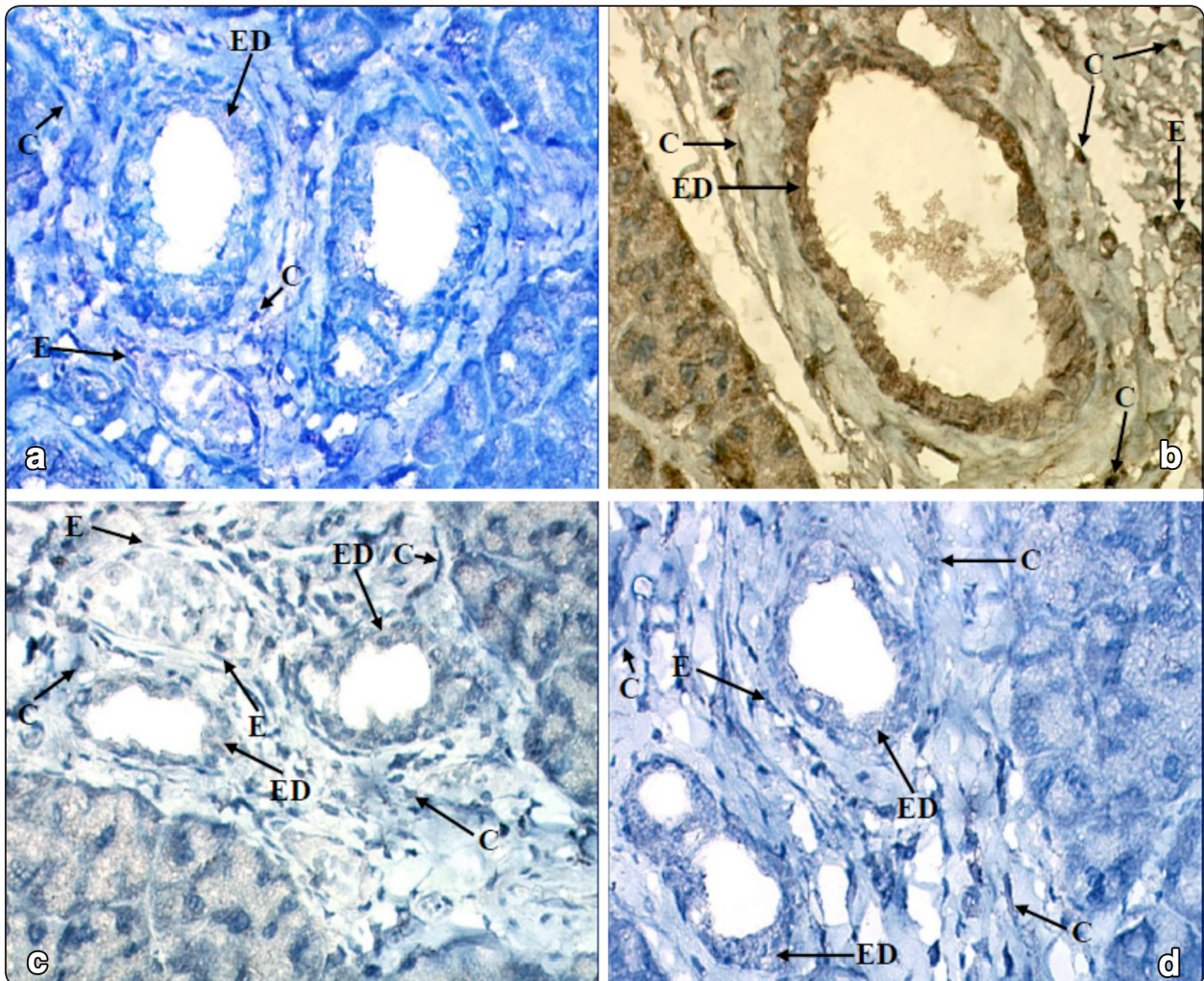


Fig. (6): Photomicrographs of caspase-3 immunolocalization: (a)- Control group (I) showing: negative nuclear immunohistochemical expression for caspase-3 but mild expression in the cytoplasm of few cells in the excretory ducts (ED), the C.T (C) as well as the endothelium (E), (the original magnification x400). (b)- Diabetic untreated group (II) showing: a strong immuno-expression for caspase-3 in the nuclei and cytoplasm of excretory duct cells (ED), the C.T cells (C) as well as the endothelial cells (E), (the original magnification x400). (c)- Insulin treated group (III) showing: moderate immuno-expression in most of the nuclei and in the cytoplasm of the excretory duct cells (ED), the C.T cells (C) as well as the endothelial cells (E), (the original magnification x400). (d)- Cod liver oil treated group (IV) showing: negative nuclear immuno-expression for caspase-3 but mild immuno-expression in the cytoplasm of the excretory duct cells (ED), the C.T cells (C) as well as the endothelial cells (E), (the original magnification x400).

Fluorescence staining results

In Group I, the secretory acini, duct system, C.T as well as the endothelium lining the BVs showed faint fluorescence with thioflavin-T stain (**Figs. 7a, 8a & 9a**). On contrary, in Group II diffuse intracellular strong fluorescence with thioflavin-T was observed in the acinar and ductal cells as well as in the endothelium. Furthermore, the C.T surrounding the

excretory ducts showed diffuse strong fluorescence. Moreover, the basement membranes of the striated ducts and the luminal membranes of both the striated and excretory ducts showed strong fluorescence. In addition, the stagnated salivary secretion in the lumina of both the striated and excretory ducts showed strong fluorescence with thioflavin-T (**Figs. 7b, 8b & 9b**). In Group III, diffuse intracellular

moderate fluorescence with thioflavin-T was observed in some acinar and ductal cells as well as in the endothelium. The C.T surrounding the excretory ducts showed moderate fluorescence except in scattered areas which showed strong fluorescence. Moreover, the basement membranes of the striated ducts and the luminal membranes of both the striated and excretory ducts showed moderate fluorescence. Furthermore, the stagnated salivary secretion in the lumina of some striated ducts showed moderate

fluorescence with thioflavin-T (**Figs. 7c, 8c & 9c**). On the other hand, in Group IV diffuse intracellular mild fluorescence with thioflavin-T was observed in some acinar and ductal cells as well as in the endothelium. Furthermore, the C.T surrounding the excretory ducts showed diffuse mild fluorescence. Moreover, the basement membranes of the striated ducts and the luminal membranes of both the striated and excretory ducts showed mild fluorescence with thioflavin-T (**Figs. 7d, 8d & 9d**).

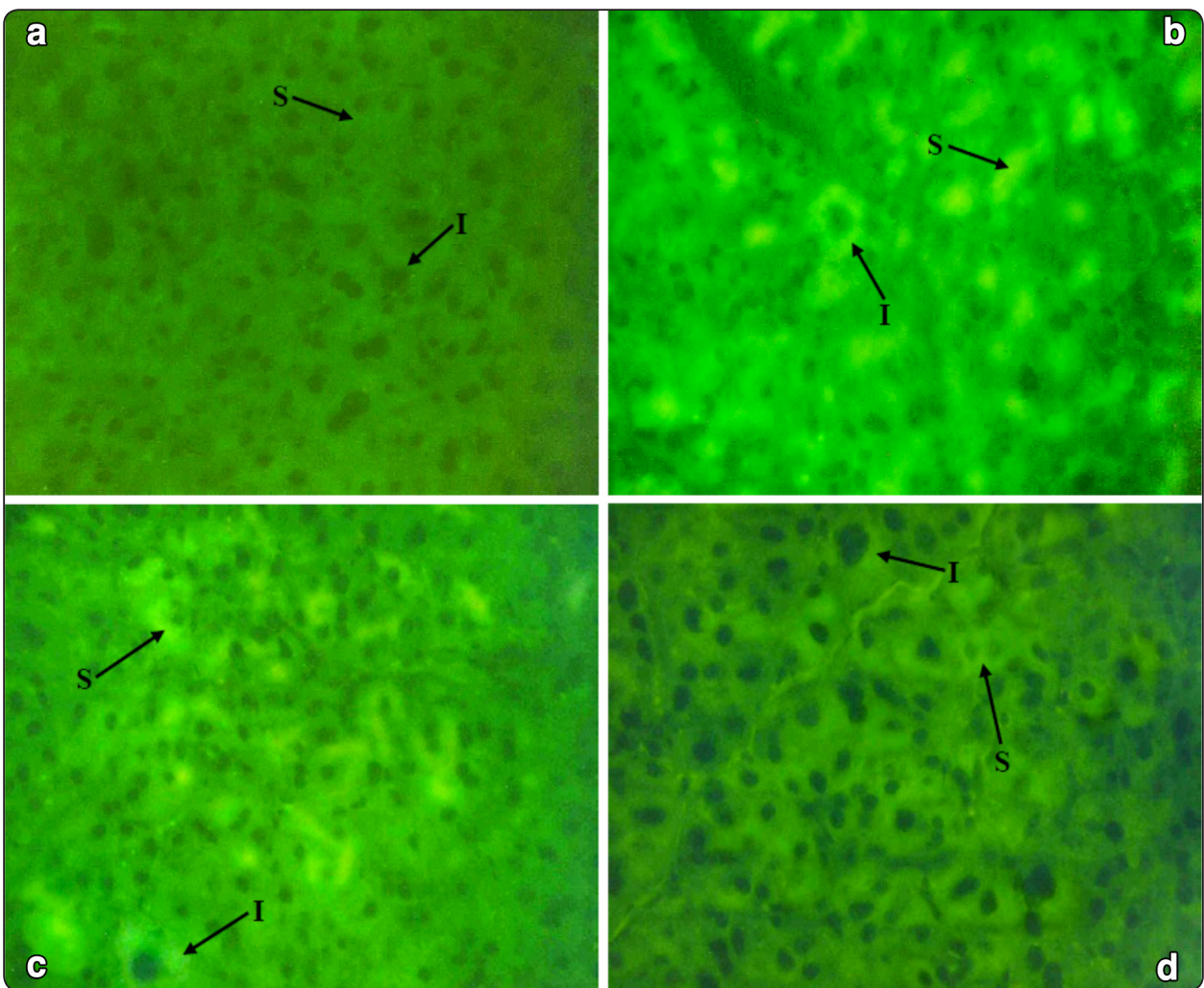


Fig. (7): Photomicrographs of thioflavin-T fluorescence staining: (a)- Control group (I) showing: the secretory acini (S) and intercalated duct cells (I) have faint fluorescence with thioflavin-T stain, (the original magnification x400). (b)- Diabetic untreated group (II) showing: diffuse intracellular strong fluorescence with thioflavin-T in the acinar (S) and intercalated duct cells (I), (the original magnification x400). (c)- Insulin treated group (III) showing: diffuse intracellular moderate fluorescence with thioflavin-T in some acinar (S) and intercalated duct cells (I), (the original magnification x400). (d)- Cod liver oil treated group (IV) showing: diffuse intracellular mild fluorescence with thioflavin-T in some acinar (S) and intercalated duct cells (I), (the original magnification x400).

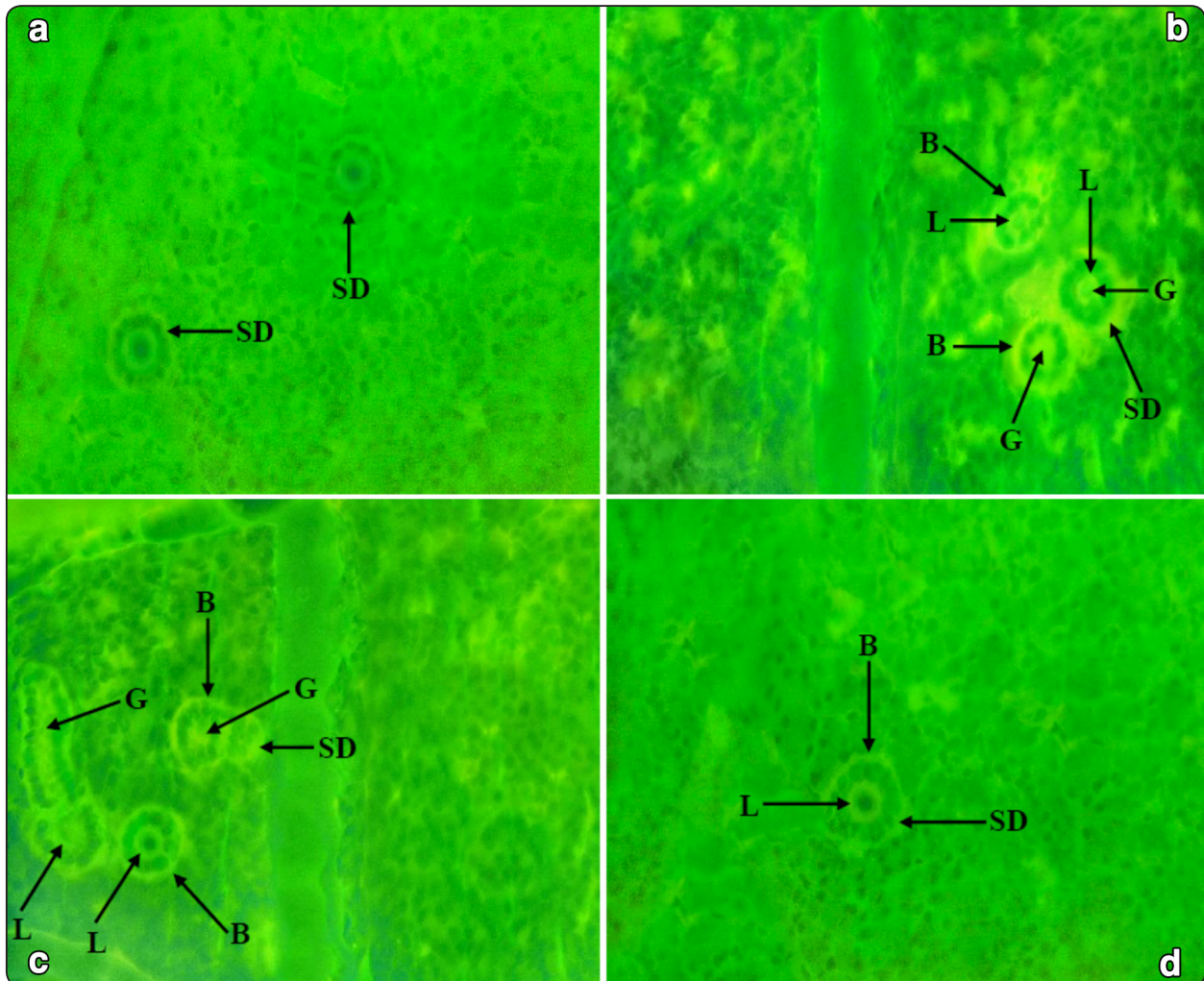


Fig. (8): Photomicrographs of thioflavin-T fluorescence staining: (a)- Control group (I) showing: the striated ducts (SD) have faint fluorescence with thioflavin-T stain, (the original magnification x400). (b)- Diabetic untreated group (II) showing: diffuse intracellular strong fluorescence with thioflavin-T in the striated duct cells (SD). Strong fluorescence in the basement membranes (B) and luminal membranes (L) of the striated ducts. In addition, the stagnated salivary secretion (G) in the lumina of the striated ducts shows strong fluorescence with thioflavin-T, (the original magnification x400). (c)- Insulin treated group (III) showing: diffuse intracellular moderate fluorescence with thioflavin-T in some striated duct cells (SD). Moderate fluorescence in the basement membranes (B) and luminal membranes (L) of the striated ducts. Furthermore, the stagnated salivary secretion (G) in the lumina of some striated ducts shows moderate fluorescence with thioflavin-T, (the original magnification x400). (d)- Cod liver oil treated group (IV) showing: diffuse intracellular mild fluorescence with thioflavin-T in some striated duct cells (SD). Mild fluorescence in the basement membrane (B) and luminal membrane (L) of the striated duct, (the original magnification x400).

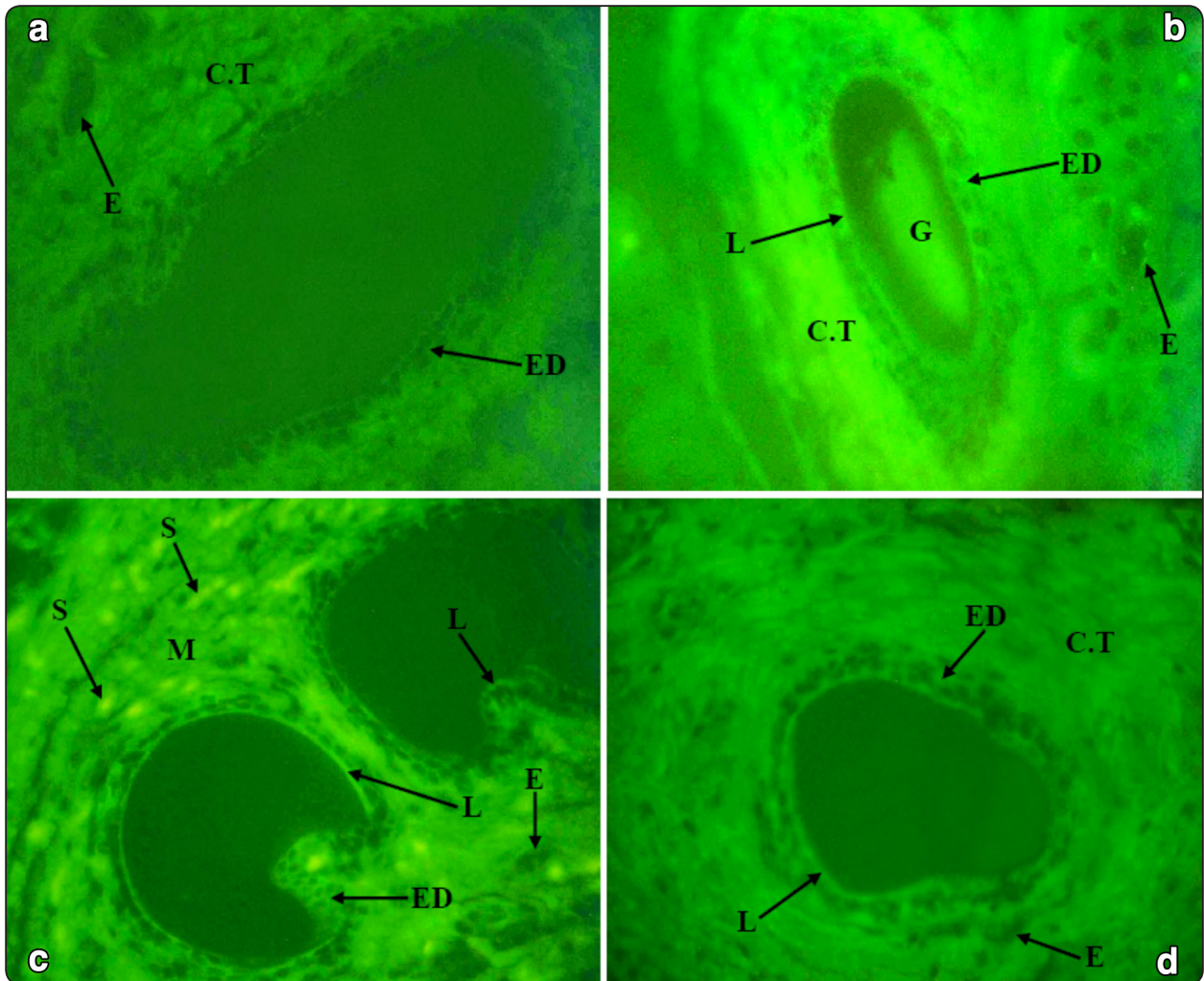


Fig. (9): Photomicrographs of thioflavin-T fluorescence staining: (a)- Control group (I) showing: the excretory duct (ED), C.T as well as the endothelium lining the BVs (E) have faint fluorescence with thioflavin-T stain, (the original magnification x400). (b)- Diabetic untreated group (II) showing: diffuse intracellular strong fluorescence with thioflavin-T in the excretory duct cells (ED) as well as in the endothelium (E). The C.T shows diffuse strong fluorescence. The luminal membrane (L) of the excretory duct shows strong fluorescence. The stagnated salivary secretion (G) in the lumen of the excretory duct shows strong fluorescence with thioflavin-T, (the original magnification x400). (c)- Insulin treated group (III) showing: diffuse intracellular moderate fluorescence with thioflavin-T in some excretory duct cells (ED) as well as in the endothelium (E). The C.T shows moderate fluorescence (M) except in scattered areas which show strong fluorescence (S). The luminal membranes (L) of the excretory ducts show moderate fluorescence with thioflavin-T, (the original magnification x400). (d)- Cod liver oil treated group (IV) showing: diffuse intracellular mild fluorescence with thioflavin-T in some excretory duct cells (ED) as well as in the endothelium (E). The C.T shows diffuse mild fluorescence. The luminal membrane (L) of the excretory duct shows mild fluorescence with thioflavin-T, (the original magnification x400).

Statistical results

a) Acinar area fraction (%)

The control group showed the highest mean acinar area fraction followed by CLO treated group, then insulin treated group and the least value was

for the diabetic untreated group. One-way ANOVA showed highly significant difference between the studied groups. Tukey's post hoc test showed highly significant difference between each group when compared with the others (table 1 & fig. 10).

TABLE (1) Showing the mean \pm SD values and results of ANOVA as well as Tukey's post hoc tests for the comparison between the studied groups regarding acinar area fraction (%).

Acinar area fraction (%)	Control	Diabetes	Insulin	Cod liver oil	ANOVA	p-value
Mean	98.52 ^a	76.51 ^b	92.02 ^c	96.71 ^d	786.962	<0.001**
\pm SD	0.15	0.24	0.11	0.10		
Min.	98.2	76	91.8	96.5		
Max.	98.7	76.9	92.2	96.9		
<i>P1</i>		<0.001**	<0.001**	<0.001**		
<i>P2</i>			<0.001**	<0.001**		
<i>P3</i>				<0.001**		

Different superscript letters in the same row indicate significant difference between each group when compared with the others according to Tukey's post hoc test.

P1: Comparison between control group versus other groups.

P2: Comparison between diabetes group versus insulin and cod liver oil groups.

P3: Comparison between insulin group versus cod liver oil group.

** : Highly significant at p-value <0.001.

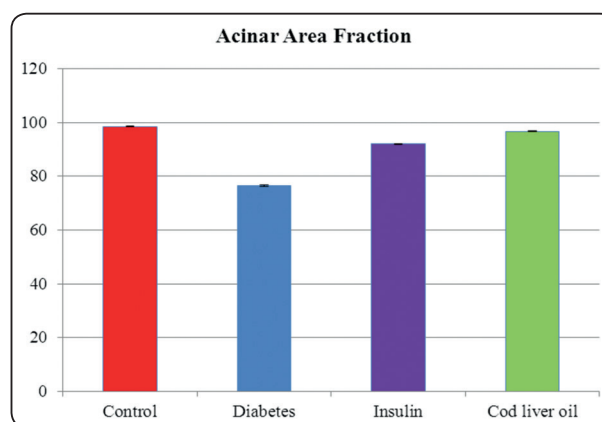


Fig. (10): Bar chart representing mean and SD values of acinar area fraction (%) in the studied groups.

b) Caspase-3 immunoreactivity

The control group showed the least mean area percentage of caspase-3 immunoreactivity followed by CLO treated group, then insulin treated group and the highest value was for the diabetic untreated

group. One-way ANOVA showed highly significant difference between the studied groups. Tukey's post hoc test showed highly significant difference between each group when compared with the others (table 2 & fig. 11).

TABLE (2) Showing the mean ± SD values and results of ANOVA as well as Tukey’s post hoc tests for the comparison between the studied groups regarding caspase-3 immunoreactivity area %.

Caspase-3 immunoreactivity area %	Control	Diabetes	Insulin	Cod liver oil	ANOVA	p-value
Mean	1.03 ^a	66.00 ^b	19.01 ^c	2.63 ^d	668.604	<0.001**
±SD	0.03	0.24	0.20	0.12		
Min.	0.9	65.7	18.6	2.5		
Max.	1.06	66.3	19.3	2.8		
P1		<0.001**	<0.001**	<0.001**		
P2			<0.001**	<0.001**		
P3				<0.001**		

Different superscript letters in the same row indicate significant difference between each group when compared with the others according to Tukey’s post hoc test.

P1: Comparison between control group versus other groups.

P2: Comparison between diabetes group versus insulin and cod liver oil groups.

P3: Comparison between insulin group versus cod liver oil group.

** : Highly significant at p-value <0.001.

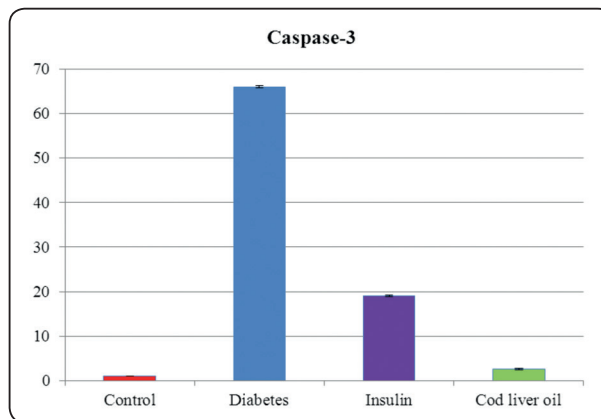


Fig. (11): Bar chart representing mean and SD values of caspase-3 immunoreactivity area % in the studied groups.

c) *Thioflavin-T assay*

The control group showed the least mean area percentage of thioflavin-T fluorescence followed by CLO treated group, then insulin treated group and the highest value was for the diabetic untreated

group. One-way ANOVA showed highly significant difference between the studied groups. Tukey’s post hoc test showed highly significant difference between each group when compared with the others (table 3 & fig. 12).

TABLE (3) Showing the mean \pm SD values and results of ANOVA as well as Tukey's post hoc tests for the comparison between the studied groups regarding thioflavin-T fluorescence area %.

Thioflavin-T fluorescence area %	Control	Diabetes	Insulin	Cod liver oil	ANOVA	p-value
Mean	0.09 ^a	39.97 ^b	19.05 ^c	1.39 ^d	524.811	<0.001**
\pm SD	0.01	0.10	0.19	0.09		
Min.	0.07	39.8	18.8	1.3		
Max.	0.11	40.1	19.3	1.5		
P1		<0.001**	<0.001**	<0.001**		
P2			<0.001**	<0.001**		
P3				<0.001**		

Different superscript letters in the same row indicate significant difference between each group when compared with the others according to Tukey's post hoc test.

P1: Comparison between control group versus other groups.

P2: Comparison between diabetes group versus insulin and cod liver oil groups.

P3: Comparison between insulin group versus cod liver oil group.

** : Highly significant at p-value <0.001.

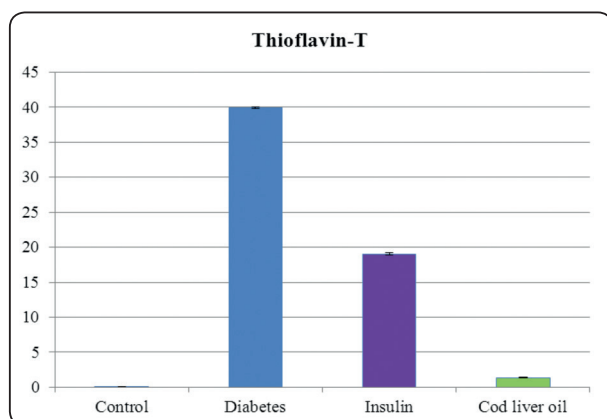


Fig. (12): Bar chart representing mean and SD values of thioflavin-T fluorescence area % in the studied groups.

DISCUSSION

The parotid gland was the gland of choice in the present study since it is similar in structure and function to the exocrine pancreas. Also when stimulated, parotid contributes with more than 50% of the total salivary secretion. Furthermore, it is known that the parotid can be more prepared to oxidative damage via reactive oxygen species (ROS)

by presenting a predominantly aerobic metabolism (Nicolau and Sasaki, 1976; Humphrey and Williamson, 2001).

One of the objectives of this study was to develop a rat model for type 2 diabetes that may mimic the clinical pathogenesis seen in humans who have insulin resistance and partial pancreatic β -cell dysfunction. This model was achieved by injection of 40 mg/kg body weight STZ which is the ideal dose for development of animal model with type 2 diabetes (Islam and Loots, 2009).

The current study revealed varying changes in the glandular architecture including changes in the acini, ducts, C.T stroma and BVs in the diabetic untreated group (Group II). The histological changes in Group II revealed nuclear changes in form of; pleomorphism, hyperchromatism, pyknosis, karyorrhexis, karyolysis and marginated chromatin. Moreover, some acinar and ductal cells degeneration was reported. Loss of the basal striations in some striated duct cells, desquamated cells in the ducts lumina as well as dilated BVs with swollen

endothelial cells were noticed. These findings are considered as pre-necrotic changes that are relevant to the persistent hyperglycemia (*Parlak et al., 2014; Shredah and El-Sakhawy, 2014*).

Ill-defined acinar and ductal cells outlines detected in Group II of this study could be attributed to the fact that among all biomolecules, lipids are the most sensitive to free radicals. Double bonds in fatty acids form peroxide products by reacting with free radicals and lipid radicals can be formed subsequently upon removal of electrons. Thus the free radicals produced in persistent hyperglycemia can elicit changes in the acyl fatty acids composition in the parotid gland. Acyl fatty acids are the main components of the phospholipid bilayer thus they form the major constituents of the biological membranes. Changes in the phospholipid fatty acid composition of acinar and ductal cell membranes will result in changes in the collective physicochemical properties of the bilayer, such as flexibility and integrity (*Mahay et al., 2004; Leite et al., 2014*).

Lipid droplets are one of the apparent results in the experimental groups of the current study especially Group II. Our results were in line with those of *Mahay et al. (2004)* who determined various diameters of infiltrated lipid droplets in the diabetic parotid tissue and reported that this was related with carbohydrate and/or fat metabolism disorders that lead to damage of the acinar and ductal cells which in turn stimulates migration of inflammatory cells leading to initiation of apoptosis.

Our histological results revealed stagnated salivary secretion in the lumina of striated and excretory ducts of Group II. These results could be explained according to the fact that diabetes not only affects the structural elements of the gland but also affects its function (*Sabino-Silva et al., 2013*). Many authors reported changes in the sodium-glucose co-transporter 1 (SGLT1) protein expression in diabetic salivary glands. They stated that SGLT1

transports (1 glucose/2 Na⁺/264 H₂O molecules) and changes in this protein can explain alterations in the salivary secretion of diabetic rats. The authors added that considering the high capacity of SGLT1 to transport water, the increase in this protein at the luminal membrane of ductal cells in diabetic rats is in accordance with the decreased salivary flow rate. Thus, the inversely proportional regulation of the luminal SGLT1 content and the salivary flow points out that this transporter is involved in the pathophysiology of diabetic xerostomia (*Loo et al., 2002; Sabino-Silva et al., 2013*). Moreover, the SGLT1 protein was initially described in the basolateral membrane of acinar cells where it provides glucose for the cellular metabolism. Similarly, the SGLT1 expression in acinar cells has been altered in diabetes (*Tarpey et al., 1995; Sabino-Silva et al., 2010*).

Like the pancreas, the salivary parotid gland is also an exocrine gland secreting mainly α -amylase, which facilitates the initial digestion of complex carbohydrates within the oral cavity. In addition, α -amylase presents specific binding sites with affinity for microorganisms (cariogenic and periodontopathogenic), forming bacterial agglomerates diluted in saliva that are easily eliminated by swallowing and consequently suffer acid digestion by the stomach (*Mahay et al., 2004; Choi et al., 2011*). Analysis of parotid secretory function revealed a significant decrease in α -amylase release in response to noradrenaline (NA) in STZ-treated glands. This decrease in amylase release in response to NA in diabetic acinar cells may be due to the insensitivity of NA to its receptors in the basolateral membrane and/or events within the signal transduction mechanism which leads to amylase secretion (*Mahay et al., 2004*).

Parotid gland normally expresses statherin protein as secretory product. Statherin reactivity was drastically reduced in parotid samples from diabetics with respect to non-diabetics. The finding

of less reactive statherin in secretory granules suggests a diminished secretion of this protein (*Isola et al., 2008*). Many data documented that diabetes causes altered concentration of salivary proteins, some appearing reduced such as proline-rich proteins, epidermal growth factor (EGF) and salivatin, other increased such as those related with inflammatory response (*Aydin, 2007*). Reduced proteins secretion evidently reflects failures in the mechanisms that regulate proteins synthesis and sorting. As salivary glands suffer from oxidative stress triggered by diabetes, endoplasmic reticulum malfunction could be the cause of their abnormal proteins secretion (*Turner et al., 2011*). Thus, the reduced statherin and other salivary proteins production falls within the consequences of the diabetes-generated oxidative stress that could be related not only with reduced proteins synthesis but also with post-translational disorders. This finding leads to include type 2 diabetes among the so-called "conformational diseases", as Parkinson's and Alzheimer's diseases, which share the occurrence of abnormally folded proteins within the endoplasmic reticulum (*Hayden et al., 2005*). The finding of reduced statherin reactivity in salivary glands of diabetic subjects strengthens the belief that the increased risk of caries, infections and periodontal disease associated with diabetes is related with altered salivary secretion. Because of the key role of statherin in starting the enamel pellicle formation, its deficiency is expected to produce a defective pellicle, thus affecting the maintenance of tooth mineralization also its deficiency affects the maintenance of salivary calcium and phosphate supersaturation. Another outcome of statherin decrease related with its binding properties towards bacteria, should be a reduced salivary efficiency in the defense of the oral surfaces against infections (*Gibbons and Hay, 1988; Garcí'a-Godoy and Hicks, 2008*).

In the current study the histological results showed dilatation of the duct system lumina. Our

finding was in agreement with that of *Parlak et al. (2014)* who attributed this finding to the metaplasia (epithelium changes to flattened cells) of the ductal cells and to the accumulation of the salivary secretion due to glandular injury and dysfunction caused by diabetes.

The histological results of Group II in this study revealed dilated BVs; lined by swollen endothelial cells and engorged with RBCs. Furthermore, few extravasated RBCs between the acini as well as inflammatory cells infiltration in the C.T surrounding the excretory ducts were detected. Our findings could be attributed to the fact that the dilatation and congestion of the BVs might be a part of inflammatory response to bring more blood to the areas of degeneration (*Moubarak, 2008*). Moreover, during hyperglycemia, increased ROS and diacylglycerol (DAG) stimulate protein kinase C (PKC) in the vascular tissue. Both PKC and ROS cause loss of permeability that leads to swelling of the endothelium (*Evcimen and King, 2007*).

In the current study, Group II showed apparent decrease in the fibrous C.T surrounding the excretory ducts, in addition to hyalinization and degeneration that were noticed in some areas. Moreover, fibroblasts showing signs of degeneration were noticed. Our findings could be explained according to the fact that advanced glycation end-products (AGEs) induce fibroblast (the matrix producing cell) apoptosis, which is mediated through caspase-3 and signaled through both caspase-8 and caspase-9 activities leading to suppression of collagen synthesis and excessive collagenolytic activity. Not only the fibroblasts, but also the inflammatory cells undergo apoptosis which is mediated through caspase-3 (*Riedl and Shi, 2004; Alikhani et al., 2005 a*).

Our imunohistochemical results confirm our histological findings observed in Group II of the current study, in which caspase-3 antibodies revealed intense positive reaction to activated

caspase-3 in the nuclei and cytoplasm of the acinar and ductal cells, C.T cells as well as the endothelial cells. Our findings could be attributed to the fact that the toxicity of STZ is related to the inhibition of the enzyme O-GlcNAcase (N-acetyl-D-glucosaminidase) which removes protein linked GlcNAc (*Liu et al., 2000; Konrad et al., 2001; Szkudelski, 2001*). The increase in intracellular levels of proteins modified by GlcNAc results in cell death by apoptosis (*Konrad et al., 2001*). Furthermore, the metabolic disturbances associated with diabetes can lead to activation of the polyol pathway, high levels of the cytokine tumor necrosis factor (TNF)- α , the formation of AGEs, high levels of PKC as well as activation and enhanced oxidative stress (*Asnaghi et al., 2003*). The activation of these pathways may be especially important in initiating events linked to inflammation and apoptosis (*Dagher et al., 2004; Xu et al., 2004*).

There are several mechanisms that could be responsible for the higher rate of apoptosis noted in Group II of the current study. One mechanism may be through the cytokine activation of receptors with 'death domains', such as TNF receptor-1 (TNFR-1) or fas (*Alikhani et al., 2005 b*). Diabetes is associated with both enhanced TNF and fas/fas-ligand expression (*Joussen et al., 2003*). Interleukin (IL)-1 or interferon (IFN)- γ may also promote apoptosis, even though their receptors lack death domains, by altering pro-apoptotic gene expression or enhancing production of oxygen radicals (*Schroder et al., 2004*). Another mechanism is through the increased oxidative stress which is one of the common pathogenic factors of diabetes complications as it leads to the formation of excess ROS which lead to severe oxidative damage of the cell's components like lipids, proteins and DNA by inhibiting many of the enzymes involved in DNA synthesis. These pathways lead to one result which is apoptosis through activation of caspases (*Riedl and Shi, 2004*).

Caspases are synthesized as catalytically inactive zymogens and must undergo proteolytic activation during apoptosis. Initiator caspases, such as caspases-8 and 9 are required to process the executioner caspases, such as caspase-3 leading to their activation. Active caspase-3 cleaves over 40 intracellular substrates that cause cell death (*Boatright and Salvesen, 2003*). Moreover, the active caspase-3 induces activation of caspase-activated deoxyribonuclease (CAD), also called DNA fragmentation factor-40 (DFF), that is involved in degrading DNA and apoptosis in different cells which in turn lead to organ atrophy and failure (*Shredah and El-Sakhawy, 2014*). It was reported that *in vivo* AGEs induce mitochondria apoptosis, which is mediated through caspase-3 and signaled through both caspase-8 and caspase-9 activities (*Alikhani et al., 2005 a*). However interestingly, AGEs stimulate nuclear factor- $\kappa\beta$ (NF- $\kappa\beta$) activation, which is anti-apoptotic (*Wang et al., 1998*). It should be mentioned that one form of apoptosis in insulin producing cells is independent of NF- $\kappa\beta$ mediated transcription but dependent on caspase-3 activity and poly adenosine diphosphate ribose (poly ADP-ribose) polymerase-1 cleavage (*Saldeen and Welsh, 1998*).

In the present study, the mild immuno-expression for caspase-3 observed in the control group (Group I) might be attributed to the physiological cell death (*Shredah and El-Sakhawy, 2014*).

Diabetes increases the degree of both lipid peroxidation and protein glycosylation also it elevates the levels of total serum cholesterol (TC), triglycerides and low-density lipoprotein (LDL), (*Hidayat et al., 2014*). Furthermore, serum biomarkers related to type 2 diabetes seem to correlate with inflammatory responses and lipid metabolism pathways. Two of these important apolipoprotein associated serum biomarkers are serum amyloid A (SAA) and serotransferrin (TRFE). SAA is a major high-density lipoprotein (HDL), 45% of total HDL

(*Border et al., 2012*). It was reported that increased expression of SAA in serum of diabetic patients was also related to SAA related inflammatory mediator, C-reactive protein (CRP). SAA and CRP, along with other acute innate immune molecules, are known to be up-regulated in liver associated with type 2 diabetic condition. However, the level of TRFE precursor is down-regulated in diabetes. It was suggested that diabetes-related serum biomarkers, especially related apolipoproteins such as SAA and TRFE, are present in saliva. These biomarkers may be released from the serum through a salivary gland apparatus (*Li et al., 2008*).

SAA protein is the precursor for amyloid A (AA). Amyloidosis is the case in which protein aggregation produces ordered polymers that form protofilaments and then fibrils. These fibrils, regardless of the type of precursor protein, are about 10 nm in diameter (*Millucci et al., 2014*). All amyloid fibrils possess cross-beta structure and consist of one particular misfolded protein or peptide. A parallel arrangement of beta-sheets with β -strands perpendicular to the axis of the fibril appears to be the major structural feature of amyloid fibrils. Amyloidogenic proteins are stabilized by intramolecular disulfide bonds. Such structural analysis is important in order to understand the pathological function of amyloid and to find inhibitors that prevent the formation of toxic species or their interaction with targets such as cell membranes or the extracellular matrix (*Munishkina and Fink, 2007*).

Tissue damage in amyloidosis occurs through multiple mechanisms. It is not only the end-stage fibrillar deposits that produce disease since it is believed that oligomeric precursors that form doughnut-like ring structures can interact with and damage cells; these rings may even insert into membranes (*Seldin and Sanchorawala, 2006*).

AA fibril accumulation was associated with membrane lesions. In AA amyloidosis, amyloids interact with constituents of basement membranes

such as perlecan, laminin and agrin. Moreover, cytoplasmic membrane and organelle (endoplasmic reticulum, mitochondria and nuclear) membrane lesions were associated with AA amyloidosis also. Vascular abnormalities including endothelial enlargement, basement membrane modifications and vascular proliferation were noticed with amyloidosis. Moreover, evidence that such precursors are toxic comes from clinical observations that organ function can improve acutely after treatment of amyloidosis, in a time frame that is believed to be too short for resorption of fibrillar deposits (*García-García et al., 2002*).

In amyloidosis, protein folding disorder occurs so normally soluble proteins are deposited extracellularly also as insoluble fibrils, impairing tissue structure and function. Charged polyelectrolytes such as glycosaminoglycans (GAGs) are frequently found associated with the amyloid deposits in tissues. Experimental evidence indicates that they can play an active role in favoring amyloid fibril formation and stabilization. Binding of GAGs to amyloid fibrils occurs mainly through electrostatic interactions involving the negative polyelectrolyte charges and positively charged side chains residues of aggregating protein. Similarly to catalyst for reactions, GAGs favor aggregation, nucleation and amyloid fibril formation thus functioning as structural templates for the self-assembly of highly cytotoxic oligomeric precursors, rich in β -sheets, into harmful amyloid fibrils. Moreover, the GAGs amyloid promoting activity can be facilitated through specific interactions via consensus binding sites between amyloid polypeptide and GAGs molecules (*Iannuzzi et al., 2015*).

The previous facts support our fluorescence staining results of Group II. Thioflavin-T was used in the current study to detect amyloid fibrils. Thioflavin-T is a benzothiazole dye that exhibits enhanced fluorescence upon binding to amyloid

fibrils and is commonly used to diagnose amyloid fibrils, both *ex vivo* and *in vitro* (*Khurana et al., 2005*).

Although type 2 diabetes is non-insulin-dependent DM however, it was reported that over time most patients with type 2 diabetes experience progressive β -cell dysfunction and will require insulin therapy for satisfactory glycemic control (*American Diabetes Association, 2009*). In the current study, the insulin dose applied was based on the proposal that the best glycemic control was obtained with the dose 5 IU/kg body weight/day (*Pinheiro et al., 2011*).

Salivary glands are directly related with hormones. Insulin and insulin-like growth factor 1 (IGF-1) receptors exist in salivary glands particularly in the cytoplasm and plasma membrane. It was reported that STZ-induced diabetes does not alter the proportion of insulin receptors (*Rocha et al., 2000*). In the current study the histological, immunohistochemical, fluorescence and statistical results of Group III were better than those of Group II. Our results were in agreement with those of *Take et al. (2007)* who reported better structural and functional integrity of parotid gland after insulin treatment. The authors attributed their results to the fact that insulin stimulates several processes such as carbohydrate transport, protein synthesis and cholecystokinin (CCK) receptor synthesis; CCK has a role in increasing the activity of α -amylase in parotid gland. Moreover, *Take et al. (2007)* reported that insulin treatment for one week showed better fatty acids profile and lipid droplet contents of the acinar cells. The researchers attributed their results to the regulation of lipid metabolism by insulin. Furthermore, insulin stimulates the synthesis of apolipoprotein E (ApoE) mRNA that leads to decrease in the level of cholesterol. Additionally, insulin has the ability to regulate the production/release of the proinflammatory cytokines, IL-1 β and TNF- α as well as the expression of P- and E-selectin.

Insulin also modulates leukocyte migration and improves antioxidant enzymes activity (*Aziz, 2009; Martins et al., 2010*).

Our results showed that insulin did not completely inhibit the complications of diabetes. This observation was in agreement with that of *Zobali et al. (2002)* as well as *Jain et al. (2006)* who stated that insulin did not completely inhibit the abnormalities in the oxidative metabolism of the parotid glands in diabetic rats that still suffered an oxidative insult. The authors attributed their results to the fact that insulin treatment partially inhibits lipid peroxidation also it is not stringent enough to prevent excessive protein glycation, which can increase tissue oxidative stress.

The histological, immunohistochemical, fluorescence and statistical results of Group IV in the current study showed that CLO inhibited to a great extent the abnormalities in the oxidative metabolism recorded in Group II compared to the effect of insulin as observed in Group III. Our results could be attributed to the fact that ω -3 fatty acids in CLO rather than other sources of ω -3 fatty acids, not only significantly attenuate the chemically-induced DM, but also act on suppressing the production of cytokines and inhibit the production of arachidonic acid-derived eicosanoids, namely the prothrombotic thromboxane A₂ by activated platelets and the proinflammatory leukotrienes B₂ and C₄ by activated leukocytes. Furthermore, ω -3 fatty acids considerably inhibit the elevation of TNF- α , IL-1, IL-6 and CRP (*Hamdy et al., 2007; Tsitouras et al., 2008*). Moreover, ω -3 fatty acids maintain the antioxidant status in a normal range through significant increase in the activities of antioxidant enzymes such as superoxide dismutase (SOD) by up regulating gene expression of antioxidant enzymes and down regulating gene associated with production of ROS (*Soltan, 2012; Hussein et al., 2014*). Consequently, ω -3 fatty acids in turn can suppress the formation of oxygen free radicals, lipid peroxides as well as aldehydes (*Hamdy et al., 2007; Hussein et al., 2014*). In addition, ω -3 fatty acids

inhibit the increase of TC as well as LDL levels and suppress triglyceridemia mainly through enhanced triacylglycerol lipolysis, enhanced fatty acid oxidation and raised HDL-c levels. Moreover, ω -3 fatty acids possibly are acting as “fraudulent fatty acids” which can in fact activate peripheral fatty acid oxidation. Therefore, the general consequence is improved insulin sensitivity and diabetes control (*Hamdy et al., 2007*). Also, ω -3 fatty acids are indeed potent activators of peroxisome proliferator-activated receptors (PPARs) thus, they improve insulin action in liver by reducing intracellular fat (long chain CoA and DAG) content which occurs via PPARs-dependent mechanism. Such mechanism is not only responsible for enhanced fatty acid utilization but also contributes to improvement in insulin sensitivity (*Tsitouras et al., 2008*). ω -3 fatty acids may also play an important role in up regulation of insulin synthesis (by β -cells) and its subsequent transport extracellularly through inhibiting oxidative stress formation. Consequently, ω -3 fatty acids have inhibitory effect on increased plasma glucose and improve glucose utilization (*Soltan, 2012*).

It was recorded that, ω -3 fatty acids showed an expressive increase of α -amylase activity in parotid gland through stimulation of adenylate-cyclase activity (*Leite et al., 2014*).

Whether or not CLO intake can prevent type 2 diabetes development, further investigations are required.

CONCLUSIONS

This study has demonstrated that diabetes has deleterious effect on the structure and function of parotid salivary glands. Moreover, it has a major role in tissue damage through development of amyloidosis.

Insulin can't completely inhibit the complications of diabetes. However, CLO represents a unique nutritional intervention that has great potential to inhibit the abnormalities caused by diabetes.

REFERENCES

1. Alikhani, Z., Alikhani, M., Boyd, C., Nagao, K., Trackman, P. and Graves, D.: Advanced glycation end products enhance expression of pro-apoptotic genes and stimulate fibroblast apoptosis through cytoplasmic and mitochondrial pathways. *J. Biol. Chem.*; 280: 12087-12095, 2005 (a).
2. Alikhani, M., Alikhani, Z. and Graves, D.: FOXO1a functions as a master switch that regulates gene expression necessary for TNF-induced fibroblast apoptosis. *J. Biol. Chem.*; 280: 12096-12102, 2005 (b).
3. American Diabetes Association: Diagnosis and classification of diabetes mellitus. *Diab. Care*; 32: S62-S67, 2009.
4. Anu Geethan, P.K.M. and Prince, P.S.M.: Antihyperlipidemic effect of D-Pinitol on streptozotocin-induced diabetic wistar Rats. *J. Biochem. Mol. Toxic.*; 22 (4): 220-224, 2008.
5. Asnaghi, V., Gerhardinger, C., Hoehn, T., Adeboje, A. and Lorenzi, M.: A role for the polyol pathway in the early neuroretinal apoptosis and glial changes induced by diabetes in the rat. *Diabetes*; 52: 506-511, 2003.
6. Aydin, S.: A comparison of ghrelin, glucose, alpha-amylase and protein levels in saliva from diabetics. *Biochem. Mol. Biol.*; 40: 29-35, 2007.
7. Aziz, O.H.: Effect of soybean seeds alone or in combination with insulin or glibenclamide on serum lipid profiles in alloxan-induced diabetic rats. *Iraqi J. Vet. Sci.*; 23 (1): 17-23, 2009.
8. Boatright, K.M. and Salvesen, G.S.: Mechanisms of caspase activation. *Curr. Opin. Cell Biol.*; 15: 725-731, 2003.
9. Border, M.B., Schwartz, S., Carlson, J., Dibble, C.F., Kohltfarber, H., Offenbacher, S., Buse, J.B. and Bencharit, S.: Exploring salivary proteomes in edentulous patients with type 2 diabetes. *Mol. Biosys.*; 8: 1304-1310, 2012.
10. Burrows, N.R., Geiss, L.S., Engelgaum, M.M. and Acton, K.J.: Prevalence of diabetes among Native Americans and Alaska Natives, 1990-1997: an increasing burden. *Diab. Care*; 23 (12): 1770-1786, 2000.
11. Carda, C., Mosquera-Lloreda, N., Salom, L., Gomez de Ferraris, M.E. and Peydro, A.: A structural and functional salivary disorders in type 2 diabetic patients. *Oral Med. Pathol.*; 11: 309-314, 2006.

12. Chapple, I.L.C. and Genco, R.: Diabetes and periodontal diseases: consensus report of the joint EFP/AAP workshop on periodontitis and systemic diseases. *J. Periodontol.*; 84 (4): S106-S112, 2013.
13. Choi, S., Baik, J.E., Jeon, J.H., Cho, K., Seo, D.G., Kum, K.Y., et al.: Identification of Porphyromonas gingivalis lipopolysaccharide-binding proteins in human saliva. *Mol. Immunol.*; 48: 2207-2213, 2011.
14. Dagher, Z., Park, Y.S., Asnaghi, V., Hoehn, T., Gerhardinger, C. and Lorenzi, M.: Studies of rat and human retinas predict a role for the polyol pathway in human diabetic retinopathy. *Diabetes*; 53: 2404-2411, 2004.
15. Evcimen, N.D. and King, G.L.: The role of protein kinase C activation and the vascular complications of diabetes. *Pharmacol. Res.*; 55 (6): 498-510, 2007.
16. Fabian, T.K., Fejerdy, P. and Csermely, P.: Salivary genomics, transcriptomics and proteomics: the emerging concept of the oral ecosystem and their use in the early diagnosis of cancer and other diseases. *Curr. Genomics*; 9: 11-21, 2008.
17. García-García, M., Mourad, G., Durfort, M., García-Valero, J. and Argilés, À.: Vascular involvement and cell damage in experimental AA and clinical β_2 -microglobulin amyloidosis. *Nephrol. Dial. Transplant.*; 17 (8): 1450-1456, 2002.
18. García-Godoy, F. and Hicks, M.J.: Maintaining the integrity of the enamel surface: the role of dental biofilm, saliva and preventive agents in enamel demineralization and remineralization. *J. Am. Dent. Assoc.*; 139: 25-34, 2008.
19. Gibbons, R.J. and Hay, D.I.: Human salivary acidic proline rich proteins and statherin promote the attachment of Actinomyces viscosus LY7 to apatitic surfaces. *Infect. Immun.*; 56: 439-445, 1988.
20. Gregersen, N. and Bross, P.: Protein misfolding and cellular stress: an overview. *Methods Mol. Biol.*; 648: 3-23, 2010.
21. Hamdy, M.S., Moselhy, S.S., Makhlof, A.A. and Fathy, A.H.: Cod liver oil in chemically-induced diabetes mellitus in rats. *J. Biol. Res.*; 7: 59-65, 2007.
22. Hayden, M.R., Tyagi, S.C., Kerklo, M.M. and Nicolls, M.R.: Type 2 diabetes mellitus as a conformational disease. *JOP*; 6: 287-302, 2005.
23. Hidayat, M., Tahir, M. and Shoro, A.A.: Melatonin preserves the morphology of parotid gland damaged by streptozotocin-induced diabetes. *J. Postgrad. Med. Inst.*; 28 (2): 128-132, 2014.
24. Hirtz, C., Chevalier, F., Sommerer, N., Raingeard, I., Bringer, J., Rossignol, M. and de Pe'riere Deville, D.: Salivary protein profiling in type I diabetes using two-dimensional electrophoresis and mass spectrometry. *Clin. Proteomics*; 2: 117-127, 2006.
25. Humphrey, S.P. and Williamson, R.T.: A review of saliva: normal composition, flow and function. *J. Prosth. Dent.*; 85 (2): 162-169, 2001.
26. Hussein, J.S., El-Khayat, Z., Morsy, S., Oraby, F. and Singer, G.: The effect of fish oil on oxidant/antioxidant status in diabetic rats through the reduction of arachidonic acid in the cell membrane. *Int. J. Pharm. & Pharm. Sci.*; 6 (2): 196-199, 2014.
27. Iannuzzi, C., Irace, G. and Sirangelo, I.: The effect of glycosaminoglycans (GAGs) on amyloid aggregation and toxicity. *Molecules*; 20: 2510-2528, 2015.
28. Islam, M.S. and Loots, D.T.: Experimental rodent models of type 2 diabetes: a review. *Methods Find. Exp. Clin. Pharmacol.*; 31: 249-261, 2009.
29. Isola, M., Cabras, T., Inzitari, R., et al.: Electron microscopic detection of statherin in secretory granules of human major salivary glands. *J. Anat.*; 212: 664-668, 2008.
30. Jain, S., Pandhi, P., Singh, A.P. and Malhotra, S.: Efficacy of standardized herbal extracts in type 1 diabetes - an experimental study. *Afr. J. Trad. CAM*; 3 (4): 23-33, 2006.
31. Jorgensen, M.F., Bjergaard, P. and Barchjohansen, K.: Diabetes and impaired glucose tolerance among the Inuit population of Greenland. *Diab. Care*; 25 (10): 1766-1771, 2002.
32. Jousseaume, A.M., Poulaki, V., Mitsiades, N., Cai, W.Y., Suzuma, I., Pak, J., et al.: Suppression of Fas-FasL-induced endothelial cell apoptosis prevents diabetic blood-retinal barrier breakdown in a model of streptozotocin-induced diabetes. *FASEB J.*; 17: 76-78, 2003.
33. Khurana, R., Coleman, C., Ionescu-Zanetti, C., Carter, S.A., Krishna, V., Grover, R.K., Roy, R. and Singh, S.: Mechanism of thioflavin-T binding to amyloid fibrils. *J. Struct. Biol.*; 151 (3): 229-238, 2005.
34. Kidambi, S. and Patel, S.B.: Diabetes mellitus: considerations for dentistry. *J. Am. Dent. Assoc.*; 139: 8-18, 2008.

35. Konrad, R.J., Mikolaenko, I., Tolar, J.F., Liu, K. and Kudlow, J.E.: The potential mechanism of the diabetogenic action of streptozotocin: inhibition of pancreatic β -cell O-GlcNAc-selective N-acetyl- β -D-glucosaminidase. *Biochem. J.*; 356: 31-41, 2001.
36. Leite, M.F., Lima, A.M., Sun Kang, S.J., Santos, M.T. and Otton, R.: Effect of astaxanthin and fish oil on enzymatic antioxidant system and α -amylase activity of salivary glands from rats. *Braz. J. Oral Sci.*; 13 (1): 58-63, 2014.
37. Li, R.X., Chen, H.B., Tu, K., Zhao, S.L., Zhou, H., Li, S.J., Dai, J., Li, Q.R., Nie, S., Li, Y.X., Jia, W.P., Zeng, R. and Wu, J.R.: Localized-statistical quantification of human serum proteome associated with type 2 diabetes. *PLOS One*; 3 (9): 1-13, 2008.
38. Liu, K., Paterson, A.J., Chin, E. and Kudlow, J.E.: Glucose stimulates protein modification by O-linked GlcNAc in pancreatic β cells: linkage of O-linked GlcNAc to β cell death. *Proc. Natl. Acad. Sci. USA*; 97: 2820-2825, 2000.
39. Loo, D.D., Wright, E.M. and Zeuthen, T.: Water pumps. *J. Physiol.*; 542: 53-60, 2002.
40. Lordan, S., Ross, R.P. and Stanton, C.: Marine bioactives as functional food ingredients: potential to reduce the incidence of chronic diseases. *Mar. Drugs*; 9: 1056-1100, 2011.
41. Mahay, S., Adeghate, E., Lindley, M.Z., Rolph, C.E. and Singh, J.: Streptozotocin-induced type 1 diabetes mellitus alters the morphology, secretory function and acyl lipid contents in the isolated rat parotid salivary gland. *Mol. Cell. Biochem.*; 261: 175-181, 2004.
42. Marjan, A., Shariar, E., Rouhollah, H., Jalaledin, M., Habibolah, P., et al.: Effect of short and long-term treatment with omega-3 fatty acids on scopolamine-induced amnesia. *Iranian J. Pharm. Res.*; 11: 533-540, 2012.
43. Martins, J.O., Campos, C.A., Cruz, W.M.C., Manzolli, S., Alves, A.F., Vianna, E.O., Jancar, S. and Sannomiya, P.: Insulin modulates cytokine release and selectin expression in the early phase of allergic airway inflammation in diabetic rats. *BMC Pulm. Med.*; 10: 1-9, 2010.
44. Mckim, S.E., Kono, A., Gabele, E., Uesugi, T., Froh, M., Sies, H., Thurman, R.G. and Arteel, G.E.: Cocoa extract protects against early alcohol induced liver injury in the rat. *Arch. Biochem. Bioassay*; 406: 40-46, 2002.
45. Merlini, G. and Bellotti, V.: Molecular mechanisms of amyloidosis. *N. Engl. J. Med.*; 349: 583-596, 2003.
46. Millucci, L., Ghezzi, L., Bernardini, G., Braconi, D., Lupetti, P., Perfetto, F., Orlandini, M. and Santucci, A.: Diagnosis of secondary amyloidosis in alkaptonuria. *Diagn. Pathol.*; 9: 1-9, 2014.
47. Moubarak, R.: The effect of hypercholesterolemia on the rat parotid salivary glands (histopathological and immunohistochemical study). *CDJ*; 24 (I): 19-28, 2008.
48. Munishkina, L.A. and Fink, A.L.: Fluorescence as a method to reveal structures and membrane-interactions of amyloidogenic proteins. *Biochim. Biophys. Acta*; 1768: 1862-1885, 2007.
49. Negrato, C.A. and Tarzia, O.: Buccal alterations in diabetes mellitus. *Diabetol. Metab. Syndr.*; 15: 1-11, 2010.
50. Nicolau, J. and Sasaki, K.T.: Metabolism of carbohydrate in the major salivary glands of the rats. *Arch. Oral Biol.*; 21: 659-661, 1976.
51. Obici, L., Perfetti, V., Palladini, G., Moratti, R. and Merlini, G.: Clinical aspects of systemic amyloid diseases. *Biochim. Biophys. Acta*; 1753: 11-22, 2005.
52. Parlak, S.N., Tatar, A., Keles, O.N., Selli, J., Can, I. and Unal, B.: Effects of menopause and diabetes on the rat parotid glands: a histopathological and stereological study. *Int. J. Med. Sci. Pub. H.*; 3 (6): 749-755, 2014.
53. Pinheiro, L.S., Melo, A.D., Andreazzi, A.E., Júnior, L.C.C., Costa, M.B. and Garcia, R.M.G.: Protocol of insulin therapy for streptozotocin-diabetic rats based on a study of food ingestion and glycemic variation. *Scand. J. Lab. Anim. Sci.*; 38 (2): 117-127, 2011.
54. Rao, P.V., Reddy, A.P., Lu, X., Dasari, S., Krishnaprasad, A., Biggs, E., Roberts, C.T. and Nagalla, S.R.: Proteomic identification of salivary biomarkers of type-2 diabetes. *J. Proteome Res.*; 8: 239-245, 2009.
55. Riedl, S.J. and Shi, Y.: Molecular mechanisms of caspase regulation during apoptosis. *Nat. Rev. Mol. Cell Biol.*; 5: 897-907, 2004.
56. Rocha, E.M., De Mlima, M.H., Carvalho, C.R., Saad, M.J. and Velloso, L.A.: Characterization of the insulin-signaling pathway in lacrimal and salivary glands of rats. *Curr. Eye Res.*; 21: 833-842, 2000.
57. Sabino-Silva, R., Alves-Vagner, A.B.T., Burgi, K., Okamoto, M.M., Alves, A.S., Lima, G.A., Freitas, H.S., Antunes, V.R. and Machado, U.F.: SGLT1 protein expression in plasma membrane of acinar cells correlates with the sympathetic outflow to salivary glands in diabetic

- and hypertensive rats. *Am. J. Physiol. Endocrinol. Metab.*; 299: 1028-1037, 2010.
58. Sabino-Silva, R., Okamoto, M.M., David-Silva, A., Mori, R.C., Freitas, H.S. and Machado, U.F.: Increased SGLT1 expression in salivary gland ductal cells correlates with hyposalivation in diabetic and hypertensive rats. *Diabetol. Metab. Syndr.*; 5: 64-68, 2013.
59. Saldeen, J. and Welsh, N.: Nicotinamide-induced apoptosis in insulin producing cells is associated with cleavage of poly (ADP-ribose) polymerase. *Mol. Cell. Endocrinol.*; 139: 99-107, 1998.
60. Schroder, K., Hertzog, P., Ravasi, T. and Hume, D.: Interferon-gamma: an overview of signals, mechanisms and functions. *J. Leukocyte Biol.*; 75: 163-189, 2004.
61. Seldin, D.C. and Sancharawala, V.: Editorials and perspectives: adapting to AL amyloidosis. *Hematol. J.*; 91 (12): 1591-1595, 2006.
62. Shen, D., Coleman, J., Chan, E., Nicholson, T.P., Dai, L., Sheppard, P.W. and Patton, W.F.: Novel cell- and tissue-based assays for detecting misfolded and aggregated protein accumulation within aggresomes and inclusion bodies. *Cell Biochem. Biophys.*; 60: 173-185, 2011.
63. Shredah, M. and El-Sakhawy, M.A.: Immunohistochemical expression of activated caspase-3 in the parotid salivary glands of rats after long administration of *Myristica fragrans*. *Int. J. Adv. Res.*; 2 (12): 493-499, 2014.
64. Simonsen, T., Vartun, F.A., Lyngmo, V. and Nordoy, A.: A coronary heart disease, serum lipid, platelets and dietary fish in two communities in Northern Norway. *Acta Medica Scand.*; 222 (3): 237-243, 1987.
65. Skinner, M., Sancharawala, V., Seldin, D.C., Dember, L.M., Falk, R.H., Berk, J.L., Anderson, J.J., O'Hara, C., Finn, K.T., Libbey, C.A., Wiesman, J., Quillen, K., Swan, N. and Wright, D.G.: High-dose melphalan and autologous stem-cell transplantation in patients with AL amyloidosis: an 8-year study. *Ann. Intern. Med.*; 140: 85-93, 2004.
66. Soltan, S.A.: The effects of varieties sources of omega-3 fatty acids on diabetes in rats. *Food Nutr. Sci.*; 3: 1404-1412, 2012.
67. Szkudelski, T.: The mechanism of alloxan and streptozotocin action in β cells of the rat pancreas. *Physiol. Res.*; 50: 536-546, 2001.
68. Take, G., Ilgaz, C., Erdogan, D., Ozogul, C. and Elmas, C.: A comparative study of the ultrastructure of submandibular, parotid and exocrine pancreas in diabetes and fasting. *SMJ*; 28 (1): 28-35, 2007.
69. Tarpey, P.S., Wood, I.S., Shirazi-Beechey, S.P. and Beechey, R.B.: Amino acid sequence and the cellular location of the Na (+)-dependent D-glucose symporters (SGLT1) in the ovine enterocyte and the parotid acinar cell. *Biochem. J.*; 312: 293-300, 1995.
70. Tsitouras, P.D., Gucciardo, F., Salbe, A.D., Heward, C. and Harman, S.M.: High omega-3 fat intake improves insulin sensitivity and reduces CRP and IL6, but does not affect other endocrine axes in healthy older adults. *Horm. Metab. Res.*; 40: 199-205, 2008.
71. Turner, S., Zettler, G., Arcos, M.L., Cremaschi, G., Davicino, R. and Anesini, C.: Effect of streptozotocin on reactive oxygen species and antioxidant enzyme secretion in rat submandibular glands: a direct and an indirect relationship between enzyme activation and expression. *Eur. J. Pharmacol.*; 659: 281-288, 2011.
72. Wang, C., Mayo, M., Korneluk, R., Goeddel, D. and Baldwin, A.J.: NF-kappaB antiapoptosis: induction of TRAF1 and TRAF2 and c-IAP1 and c-IAP2 to suppress caspase-8 activation. *Science*; 281: 1680-1683, 1998.
73. Westermark, P., Benson, M.D., Buxbaum, J.N., Cohen, A.S., Frangione, B., Ikeda, S., Masters, C.L., Merlini, G., Saraiva, M.J. and Sipe, J.D.: Amyloid: toward terminology clarification. Report from the Nomenclature Committee of the International Society of Amyloidosis. *Amyloid*; 12: 1-4, 2005.
74. Wong, D.T.: Salivary diagnostics powered by nanotechnologies, proteomics and genomics. *J. Am. Dent. Assoc.*; 137: 313-321, 2006.
75. Xu, X., Zhu, Q., Xia, X., Zhang, S., Gu, Q. and Luo, D.: Blood-retinal barrier breakdown induced by activation of protein kinase C via vascular endothelial growth factor in streptozotocin-induced diabetic rats. *Curr. Eye Res.*; 28: 251-256, 2004.
76. Zobali, F., Avci, A., Canbolat, O. and Karasu, C.: Effects of vitamin A and insulin on the antioxidative state of diabetic rat heart: a comparison study with combination treatment. *Cell Biochem. Funct.*; 20 (2): 75-80, 2002.